MASTERING MEMORY TASKS WITH WORLD MODELS

Mohammad Reza Samsami[*1,2] **Artem Zholus**[*1,3] **Janarthanan Rajendran**[1,2]
Sarath Chandar[1,3,4]

[1]Mila – Quebec AI Institute [2]Université de Montréal [3]Polytechnique Montréal [4]CIFAR AI Chair

ABSTRACT

Current model-based reinforcement learning (MBRL) agents struggle with long-term dependencies. This limits their ability to effectively solve tasks involving extended time gaps between actions and outcomes, or tasks demanding the recalling of distant observations to inform current actions. To improve temporal coherence, we integrate a new family of state space models (SSMs) in world models of MBRL agents to present a new method, Recall to Imagine (R2I). This integration aims to enhance both long-term memory and long-horizon credit assignment. Through a diverse set of illustrative tasks, we systematically demonstrate that R2I establishes a new state-of-the-art performance in challenging memory and credit assignment RL tasks, such as Memory Maze, BSuite, and POPGym. At the same time, it upholds comparable performance in classic RL tasks, such as Atari and DMC, suggesting the generality of our method. We also show that R2I is faster than the state-of-the-art MBRL method, DreamerV3, resulting in faster wall-time convergence.

1 INTRODUCTION

In reinforcement learning (RL), *world models* (Kalweit & Boedecker, 2017; Ha & Schmidhuber, 2018; Hafner et al., 2019b), which capture the dynamics of the environment, have emerged as a powerful paradigm for integrating agents with the ability to perceive (Hafner et al., 2019a; 2020; 2023), simulate (Schrittwieser et al., 2020; Ye et al., 2021; Micheli et al., 2023), and plan (Schrittwieser et al., 2020) within the learned dynamics. In current model-based reinforcement learning (MBRL), the agent **learns** the world model from past experiences, enabling it to "imagine" the consequences of its actions (such as the future environment rewards and observations) and make informed decisions.

However, MBRL introduces a key challenge: learning a world model capable of accurately simulating the environment's evolution, including the prediction of future rewards, while incorporating the agent's action policy over extended time horizons. This challenge is related to and further magnified by the credit assignment (CA) problem, which is the problem of measuring an action's influence on future rewards. The agent also may need to memorize and subsequently recall past experiences to infer optimal actions. This intertwined challenge of long-term memory and CA frequently arises as a result of inadequate learning of long-range dependencies (Ni et al., 2023). This deficiency is primarily due to constraints in currently used world models' backbone network architecture.

More specifically, Recurrent Neural Networks (RNNs; Hochreiter & Schmidhuber (1997); Cho et al. (2014)) are employed in most MBRL methods (Ha & Schmidhuber, 2018; Hafner et al., 2019b;a; 2020; 2023) as the world models' backbone architecture because of their ability to handle sequential data. However, their efficacy is hindered by the vanishing gradients (Bengio et al., 1994; Pascanu et al., 2013; Veit et al., 2016). Alternately, due to the remarkable achievements of Transformers (Vaswani et al., 2017) in language modeling tasks (Brown et al., 2020; Thoppilan et al., 2022), they have been recently adopted to build world models (Chen et al., 2022; Micheli et al., 2023; Robine et al., 2023). Nonetheless, the computational complexity of Transformers is quadratic in its input sequence length. Even the optimized Transformers (Dai et al., 2019; Wang et al., 2020; Zaheer et al., 2021; Choromanski et al., 2022; Bulatov et al., 2022; Ding et al., 2023) become unstable during

[*]these authors contributed equally to this work, the order is determined by a coin toss.
Correspondence to: {mohammad-reza.samsami, artem.zholus}@mila.quebec

training on long sequences (Zhang et al., 2022). This prohibits Transformers-based world models from scaling to long input sequence lengths that might be required in certain RL tasks.

Recent studies have revealed that state space models (SSMs) can capture dependencies in tremendously long sequences for supervised learning (SL) and self-supervised learning (SSL) tasks (Gu et al., 2021a; Nguyen et al., 2022; Mehta et al., 2022; Smith et al., 2023; Wang et al., 2023). More specifically, the S4 model (Gu et al., 2021a) redefined the long-range sequence modeling research landscape by mastering highly difficult benchmarks (Tay et al., 2020). The S4 model is derived from a time-invariant linear dynamical system where state matrices are learned (Gu et al., 2021b). In SL and SSL tasks, it exhibits a remarkable capability to capture dependencies extending up to 16K in length, surpassing the limitations of all prior methods. Given these achievements and MBRL methods' limitations in solving memory and CA tasks, the adoption of S4 or a modified version of it is a logical decision. In this paper, we introduce a novel method termed *Recall to Imagine* (R2I), which is the first MBRL approach utilizing a variant of S4 (which was previously employed in model-free RL (David et al., 2023; Lu et al., 2023)). This method empowers agents with long-term memory. R2I emerges as a general and computationally efficient approach, demonstrating state-of-the-art (SOTA) performance in a range of memory domains. We conduct experiments using the best-performing baselines and demonstrate that R2I can outperform them on tasks that require long-term memory or credit assignment while maintaining commendable performance across other benchmarks. Our contributions can be summarized as follows:

- We introduce R2I, a memory-enhanced MBRL agent built upon DreamerV3 (Hafner et al., 2023) that uses a modification of S4 to handle temporal dependencies. R2I inherits the generality of DreamerV3, operating with fixed world model hyperparameters on every domain, while also offering an improvement in computational speed of up to 9 times.
- We demonstrate SOTA performance of the R2I agent in a diverse set of memory domains: POPGym (Morad et al., 2023), Behavior Suite (BSuite; Osband et al. (2020)), both representing simplistic RL tasks requiring memory, and Memory Maze (Pasukonis et al., 2022), a challenging 3D environment with extremely long-term memory needed to be solved.
- We investigate R2I's performance in established RL benchmarks, namely Atari (Bellemare et al., 2013) and DMC (Tassa et al., 2018). We show that R2I's improved memory does not compromise performance across different types of control tasks, highlighting its generality.
- We conduct ablation experiments to show the impact of the design decisions made for R2I.

2 Background

2.1 State Space Models

A recent work (Gu et al., 2021a) has introduced a novel Structured State Space Sequence model (S4). This model has shown superior performance in SL and SSL tasks, compared to common deep sequence models, including RNNs, convolutional neural networks (CNNs; lec (1998)), and Transformers. It outperforms them in terms of both computational efficiency (Gu et al., 2021b) and the ability to model extremely long-range dependencies (Gu et al., 2020). S4 is a specific instance of state space models (SSMs), which can be efficiently trained by using specialized parameterization.

SSMs are derived from a linear dynamical system with control variable $u(t) \in \mathbb{R}$ and observation variable $y(t) \in \mathbb{R}$, utilizing state variables $x(t) \in \mathbb{C}^N$ for a state size N. The system is represented by the state matrix $\mathbf{A} \in \mathbb{C}^{N \times N}$ and other matrices $\mathbf{B} \in \mathbb{C}^{N \times 1}$, $\mathbf{C} \in \mathbb{C}^{1 \times N}$, and $\mathbf{D} \in \mathbb{R}^{1 \times 1}$:

$$x'(t) = \mathbf{A}x(t) + \mathbf{B}u(t), \quad y(t) = \mathbf{C}x(t) + \mathbf{D}u(t). \tag{1}$$

Note that these SSMs function on continuous sequences. They can be discretized by a step size Δ to allow discrete recurrent representation:

$$x_n = \bar{\mathbf{A}}x_{n-1} + \bar{\mathbf{B}}u_n, \quad y_n = \bar{\mathbf{C}}x_n + \bar{\mathbf{D}}u_n, \tag{2}$$

where $\bar{\mathbf{A}}, \bar{\mathbf{B}}, \bar{\mathbf{C}}$, and $\bar{\mathbf{D}}$ are discrete-time parameters obtained from the continuous-time parameters and Δ using methods like zero-order hold and bilinear technique (Smith et al., 2023). These representations are incorporated as a neural network layer, and each SSM is used to process a single dimension of the input sequence and map it to a single output dimension. This means that there are separate linear transformations for each input dimension, which are followed by a nonlinearity. This

allows working with discrete sequence tasks, such as language modeling (Merity et al., 2016), speech classification (Warden, 2018), and pixel-level 1D image classification (Krizhevsky et al., 2009).

S4 model characterizes $\mathbf{A}$ as a matrix with a diagonal plus low-rank (DPLR) structure (Gu et al., 2021a). One benefit of this "structured" representation is that it helps preserve the sequence history; S4 employs HiPPO framework (Gu et al., 2020) to initialize the matrix $\mathbf{A}$ with special DPLR matrices. This initialization grants the SSMs the ability to decompose $u(t)$ into a set of infinitely long basis functions, enabling the SSMs to capture long-range dependencies. Further, to make S4 more practical on modern hardware, Gu et al. (2021a) have reparameterized the mapping $u_{1:T}, x_0 \rightarrow y_{1:T}, x_T$ as a global convolution, referred to as the *convolution mode*, thereby avoiding sequential training (as in RNNs). This modification has made S4 faster to train, and as elaborated in Gu et al. (2021b), S4 models can be thought of as a fusion of CNNs, RNNs, and classical SSMs. Smith et al. (2023) uses **parallel scan** (Blelloch, 1990) to compute $u_{1:T}, x_0 \rightarrow y_{1:T}, x_{1:T}$ as efficient as **convolution mode**.

S4 has demonstrated impressive empirical results on various established SL and SSL benchmarks involving long dependencies, and it outperforms Transformers (Vaswani et al., 2017; Dao et al., 2022) in terms of inference speed and memory consumption due to its recurrent inference mode. Moreover, some recent works have focused on understanding S4 models, as well as refining them and augmenting their capabilities (Gupta et al., 2022a; Gu et al., 2022; Mehta et al., 2022; Gupta et al., 2022b; Smith et al., 2023; Ma et al., 2023). We have provided additional details in Appendix C to explain this family of S4 models. For the sake of simplicity in this study, we will be referring to all the S4 model variations as "SSMs". It is worth highlighting that a few recent methods optimize the performance of SSMs by integrating them with Transformers (Fu et al., 2023; Zuo et al., 2022; Fathi et al., 2023). This enhances the SSMs by adding a powerful local attention-based inductive bias.

2.2 From Imagination To Action

We frame a sequential decision-making problem as a partially observable Markov decision process (POMDP) with observations o_t, scalar rewards r_t, agent's actions a_t, episode continuation flag c_t, and discount factor $\gamma \in (0, 1)$, all following dynamics $o_t, r_t, c_t \sim p(o_t, r_t, c_t \mid o_{<t}, a_{<t})$. The goal of RL is to train a policy π that maximizes the expected value of the discounted return $\mathbb{E}_\pi\big[\sum_{t\geq 0} \gamma^t r_t\big]$.

In MBRL, the agent learns a model of the environment's dynamics (i.e., the world model), through an iterative process of collecting data using a policy, training the world model on the accumulated data, and optimizing the policy through the world model (Sutton, 1990; Ha & Schmidhuber, 2018). The Dreamer agent (Hafner et al., 2019a) and its subsequent versions (Hafner et al., 2020; 2023) have been impactful MBRL systems that learn the environment dynamics in a compact latent space and learn the policy entirely within that latent space. Dreamer agents consist of three primary components: the **world model**, which predicts the future outcomes of potential actions, the **critic**, which estimates the value of each state, and the **actor**, which learns to take optimal actions.

In Dreamer, an RNN-based architecture called Recurrent State-Space Model (RSSM), proposed by Hafner et al. (2019b), serves as the core of the world model, and it can be described as follows. For every time step t, it represents the latent state through the concatenation of deterministic state h_t and stochastic state z_t. Here, h_t is updated using a Gated Recurrent Unit (GRU; Cho et al. (2014)), and then is utilized to compute z_t, which incorporates information about the current observation o_t and is subsequently referred to as the posterior state. Additionally, the prior state $\hat{z}_t$ which predicts z_t without access to o_t is computed using h_t. By leveraging the latent state (z_t, h_t), we can reconstruct various quantities such as o_t, r_t, and c_t. The RSSM comprises three components: a sequence model $(h_t = f_\theta(h_{t-1}, z_{t-1}, a_{t-1}))$, a representation model $(z_t \sim q_\theta(z_t \mid h_t, o_t))$, and a dynamics model $(\hat{z}_t \sim p_\theta(\hat{z}_t \mid h_t))$, where a_{t-1} is the action at time step $t-1$, and θ denotes the combined parameter vector of all components. In addition to the RSSM, the world model has separate prediction heads for o_t, r_t, c_t. Dreamer employs an imagination-based approach to train its actor and critic components. Within this imagination phase, it harnesses the RSSM to simulate trajectories. This is performed through an iterative computation of states $\hat{z}_t, h_t$ and actions $\hat{a}_t \sim \pi(\hat{a}_t \mid \hat{z}_t, h_t)$ without the need for observations (except in the initial step). The sequences of $\hat{z}_{1:T}, h_{1:T}, \hat{a}_{1:T}$ are used to train the actor and the critic. See Appendix E for more details.

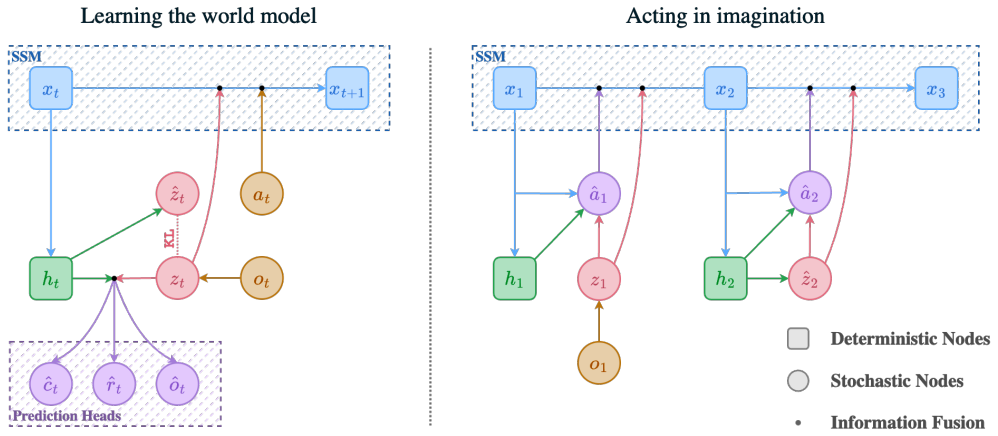

Figure 1: Graphical representation of R2I. **(Left)** The world model encodes past experiences, transforming observations and actions into compact latent states. Reconstructing the trajectories serves as a learning signal for shaping these latent states. **(Right)** The policy learns from trajectories based on latent states imagined by the world model. The representation corresponds to the full state policy, and we have omitted the critic for the sake of simplifying the illustration.

3 METHODOLOGY

We introduce R2I (Recall to Imagine), which integrates SSMs in DreamerV3's world model, giving rise to what we term the Structured State-Space Model (S3M). The design of the S3M aims to achieve two primary objectives: capturing long-range relations in trajectories and ensuring fast computational performance in MBRL. S3M achieves the desired speed through parallel computation during training and recurrent mode in inference time, which enables quick generation of imagined trajectories. In Figure 1, a visual representation of R2I is provided, and we will now proceed to describe its design.

3.1 WORLD MODEL DETAILS

Non-recurrent representation model. Our objective when updating the world model is to calculate S3M deterministic states $h_{1:T}$ in parallel by simultaneously feeding all actions a_t and stochastic state z_t, where T represents the length of the entire sequence. We aim to carry out this computation as $h_{1:T}, x_{1:T} = f_\theta((a_{1:T}, z_{1:T}), x_0)$ where x_t is a hidden state and f_θ is a sequence model with a SSM network. To achieve this, prior access to all actions $a_{1:T}$ and stochastic states $z_{1:T}$ is required. However, we encounter a challenge due to the sequential nature of the relationship between the representation model $q_\theta(z_t \mid h_t, o_t)$ and sequence model $f_\theta(h_{t-1}, z_{t-1}, a_{t-1})$: at time step t, the representation model's most recent output, denoted as z_{t-1}, is fed into the sequence model, and the resulting output h_t is then used within the representation model to generate z_t. Hence, similar to Chen et al. (2022); Micheli et al. (2023); Robine et al. (2023); Deng et al. (2023), by eliminating the dependency on h_t in the representation model, we transform it to a non-recurrent representation model $q_\theta(z_t \mid o_t)$. This modification allows us to compute the posterior samples independently for each time step, enabling simultaneous computation for all time steps. By utilizing a parallelizable function f_θ, we can then obtain $h_{1:T}$ in parallel. Appendix N includes a systematic analysis to investigate how this modification impacts the performance of the DreamerV3 across a diverse set of tasks. The results indicate that transforming $q_\theta(z_t \mid o_t, h_t)$ to $q_\theta(z_t \mid o_t)$ does not hurt the performance.

Architecture details. Inspired by Dreamer, R2I's world model consists of a representation model, a dynamics model, and a sequence model (together forming S3M). In addition to that, there are three prediction heads: an observation predictor $p_\theta(\hat{o}_t \mid z_t, h_t)$, a reward predictor $p_\theta(\hat{r}_t \mid z_t, h_t)$, and an episode continuation predictor $p_\theta(\hat{c}_t \mid z_t, h_t)$. At each time step, S3M processes a pair of (a_t, z_t) to output the deterministic state h_t. Inside, it operates over the hidden state x_t, so it can be defined as $h_t, x_t = f_\theta((a_{t-1}, z_{t-1}), x_{t-1})$. Specifically, f_θ is composed of multiple layers of SSMs, each one calculating outputs according to Equation 2. The outputs are then passed to GeLU (Hendrycks & Gimpel, 2023), which is followed by a fully-connected GLU transformation (Dauphin et al., 2017), and finally by a LayerNorm (Ba et al., 2016). This follows the architecture outlined by

Smith et al. (2023). The deterministic state h_t is the output from the final SSM layer. The set of all SSM layer hidden states is denoted x_t. See Appendix C.1 for SSMs design details. In image-based environments, we leverage a CNN encoder for $q_\theta(z_t \mid o_t)$ and a CNN decoder for $p_\theta(\hat{o}_t \mid z_t, h_t)$. In contrast, in tabular environments, both $q_\theta(z_t \mid o_t)$ and $p_\theta(\hat{o}_t \mid z_t, h_t)$ are MLPs. We include the details on network widths, depths, and other hyperparameters in Appendix F.

Training details. R2I optimizes the following objective:

$$\mathcal{L}(\theta) = \mathop{\mathbb{E}}_{z_{1:T}\sim q_\theta} \sum_{t=1}^{T} \mathcal{L}^{\text{pred}}(\theta, h_t, o_t, r_t, c_t, z_t) + \mathcal{L}^{\text{rep}}(\theta, h_t, o_t) + \mathcal{L}^{\text{dyn}}(\theta, h_t, o_t) \tag{3}$$

$$\mathcal{L}^{\text{pred}}(\theta, h_t, o_t, r_t, c_t, z_t) = -\beta_{\text{pred}}(\ln p_\theta(o_t \mid z_t, h_t) + \ln p_\theta(r_t \mid z_t, h_t) + \ln p_\theta(c_t \mid z_t, h_t)) \tag{4}$$

$$\mathcal{L}^{\text{dyn}}(\theta, h_t, o_t) = \beta_{\text{dyn}} \max(1, \mathrm{KL}[\mathtt{sg}(q_\theta(z_t \mid o_t)) \,\|\, p(z_t \mid h_t)\ ]) \tag{5}$$

$$\mathcal{L}^{\text{rep}}(\theta, h_t, o_t) = \beta_{\text{rep}} \max(1, \mathrm{KL}[\ q_\theta(z_t \mid o_t)\ \|\mathtt{sg}(p(z_t \mid h_t))\ ]) \tag{6}$$

$$h_{1:T}, x_{1:T} = f_\theta((a_{1:T}, z_{1:T}), x_0) \tag{7}$$

Here, $\mathtt{sg}$ represents the stop gradient operation. This loss, resembling the objective utilized in (Hafner et al., 2023), is derived from Evidence Lower Bound (ELBO), but our objective differs from ELBO in three ways. First, we clip KL-divergence when it falls below the threshold of 1(Hafner et al., 2020; 2023). Secondly, we use KL-balancing (Hafner et al., 2020; 2023) to prioritize the training of the S3M. Third, we use scaling coefficients $\beta_{\text{pred}}, \beta_{\text{rep}}, \beta_{\text{dyn}}$ to adjust the influence of each term in the loss function (Higgins et al., 2017; Hafner et al., 2023). Some works on SSMs recommend optimizing state matrices using a smaller learning rate; however, our experiments indicate that the most effective approach is to use the same learning rate used in the rest of the world model.

SSMs Computational Modeling. To enable the parallelizability of world model learning, as outlined in Section 2.1, we have the option to select between two distinct approaches: convolution (Gu et al., 2021a) and parallel scan (Smith et al., 2023). After thorough deliberation, we opted for parallel scan due to several compelling reasons. Firstly, as we discuss later in Section 3.2, *it is essential to pass hidden states x_t to the policy in memory environments*, a critical finding we empirically analyze in Appendix O. Another consequence of not yielding x_t via convolution mode is that it would necessitate several burn-in steps to obtain correct hidden states, akin to Kapturowski et al. (2019), resulting in quadratic imagination complexity. Furthermore, parallel scan enables scaling of sequence length in batch across distributed devices, a capability not supported by the convolution mode. Table 1 summarizes computational complexities associated with different types of recurrences, including RNNs, SSMs, and Attention used in studies like Chen et al. (2022).

Method	Training	Inference step	Imagination step	Parallel	State Reset
Attn	$\mathcal{O}(L^2)$	$\mathcal{O}(L^2)$	$\mathcal{O}((L+H)^2)$	✓	✓
RNN	$\mathcal{O}(L)$	$\mathcal{O}(1)$	$\mathcal{O}(1)$	✗	✓
SSM (Conv)	$\mathcal{O}(L)$	$\mathcal{O}(1)$	$\mathcal{O}(L)$	✓	✗
SSM (Par.Scan)	$\mathcal{O}(L)$	$\mathcal{O}(1)$	$\mathcal{O}(1)$	✓	✓

Table 1: The asymptotic runtimes of different architectures. L is the sequence length and H is the imagination horizon. The outer loop of the imagination process cannot be parallelized. Attention and SSM+Conv accept the full context of $\mathcal{O}(L+H)$ burn-in and imagined steps which results in $\mathcal{O}((L+H)^2)$ step complexity for Attention and $\mathcal{O}(L)$ for SSM+Conv. SSMs combine compact recurrence with parallel computation reaching the best asymptotical complexity.

Finally, parallel scan can facilitate the resetting of hidden states. When sampling a sequence from the buffer, it may comprise of multiple episodes; thus, the hidden states coming from terminal states to the initial states in new episodes must be reset. This boosts the early training performance, when the episodes may be short. Inspired by Lu et al. (2023), we modify the SSM inference operator to support resetting hidden states. Achieving this is not feasible with convolution mode. Details of our SSMs operator used by the parallel scan is provided in Appendix D.

3.2 Actor-Critic Details

In the design of Dreamer's world model, it is assumed that h_t contains information summarizing past observations, actions, and rewards. Then, h_t is leveraged in conjunction with the stochastic state z_t to reconstruct or predict observations, rewards, episode continuation, actions, and values. Unlike DreamerV3, which utilizes a GRU cell wherein h_t is passed both to the reconstruction heads and the next recurrent step, R2I exclusively passes h_t to prediction heads, while SSM's hidden state x_t

is used in the next recurrent update of S3M. This implies that the information stored in h_t and x_t could potentially vary. Empirically, we discovered that this difference can lead to the breakdown of policy learning when using $\pi(\hat{a}_t \mid z_t, h_t)$, but it remains intact when we use $\pi(\hat{a}_t \mid z_t, x_t)$ in memory-intensive environments. Surprisingly, we found that incorporating all features into the policy $\pi(\hat{a}_t \mid z_t, h_t, x_t)$ is not a remedy. The reason lies in the non-stationarity of these features; their empirical distribution changes over time as the world model trains, ultimately leading to instability in the policy training process. A similar phenomenon was also observed in Robine et al. (2023). We study the dependency of policy features on the performance in Appendix O, where we cover a diverse set of environments: from non-memory vector-based ones to image-based memory environments. In different environments, we condition the policy and value function on the information from S3M in the following ways: we use the *output state policy* that takes (z_t, h_t) as input, the *hidden state policy* that takes (z_t, x_t) as input, and the *full state policy* that takes (z_t, h_t, x_t) as input. To train actor-critic, we opt for the procedure proposed in DreamerV3 (Hafner et al., 2023). For a detailed description of the actor-critic training process, refer to Appendix E.

4 Experiments

We conduct a comprehensive empirical study to assess the generality and memory capacity of R2I across a wide range of domains, including credit assignment, memory-intensive tasks, and non-memory tasks, all while maintaining fixed hyperparameters of the world model. We cover five RL domains: BSuite (Osband et al., 2020), POPGym (Morad et al., 2023), Atari 100K (Łukasz Kaiser et al., 2020), DMC Tassa et al. (2018), and Memory Maze (Pasukonis et al., 2022). The section is organized as follows. In Sections 4.1 and 4.2, we evaluate R2I's performance in two distinct memory-intensive settings: simple tabular environments and complex 3D environments. Notably, we show the SOTA performance is achieved by R2I in these tasks. In Section 4.3, we demonstrate that we do not trade the generality for improved memory capabilities. **Figure 2 shows R2I's impressive computational efficiency, with a speed increase of up to 9 times compared to its predecessor, DreamerV3**. Note that the image environments are representative of Memory Maze, and the vector environments represent POPGym.

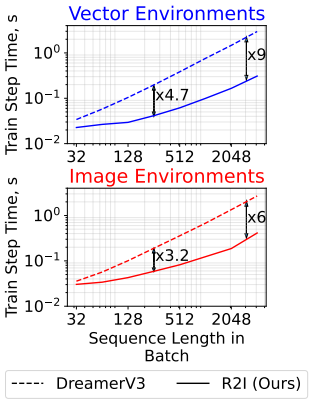

Figure 2: Computational time taken by DreamerV3 and R2I (lower is preferred)

We reuse most of the world model hyperparameters from DreamerV3. In all environments, we use a First-in First-out (FIFO) replay buffer size of 10M steps to train R2I. We found this helps stabilize the world model and prevent overfitting on a small buffer. Also, we vary features that the policy is conditioned on (i.e., output state policy $\pi(\hat{a}_t \mid z_t, h_t)$, hidden state policy $\pi(\hat{a}_t \mid z_t, x_t)$, or full state policy $\pi(\hat{a}_t \mid z_t, h_t, x_t)$). Our primary takeaway is to leverage the output state policy in non-memory environments and the full state policy or hidden state policy within memory environments, as explained in Section 3.2. We also found that even in memory environments, the full state policy cannot be preferred over the hidden state policy because of the instability of features – since the world model is trained alongside the policy, the former might change the feature distribution which introduces non-stationarity for the policy.

4.1 Quantifying Memory of R2I

In this section, we study the performance of R2I in challenging memory environments of BSuite and POPGym domains, which are tabular environments. Despite their simplicity, these environments pose a challenge for MBRL algorithms since the world model needs to learn causal connections over time. While SSMs have shown their ability to handle extremely long-range dependencies in SL and SSL (Gu et al., 2021a), this capability does not necessarily translate to MBRL, even though the world model optimizes the same supervised objective. This discrepancy arises from the lifelong nature of world model training. That is, it needs to bootstrap its performance from a very small dataset with hugely imbalanced reward "labels" (as opposed to big and well-balanced long-range datasets on which SSMs shine (Tay et al., 2021)). Additionally, the continuously growing replay buffer imposes the need to quickly learn the newly arrived data which requires an ability for quick adaptation of the

world model throughout its optimization. The section's goal is to give an insight into how extensive are R2I's memory capabilities.

Behavior Suite experiments. To study the ability of the R2I model to handle longer episodes, we conduct quantitative experiments within a subset of the BSuite environments. These environments are specifically designed to evaluate an agent's memory capacity and its ability to effectively perform credit assignment. In particular, we carry out experiments within `Memory Length` and `Discounting Chain` environments. The former focuses on memory, and the latter serves as a credit assignment task. In `Memory Length` environment, the goal is to output an action which is dictated by the initial observation (the episode length i.e., the *memory steps number* is an environment parameter). Essentially, the agent must carry the information from the initial observation throughout the entire episode. In the `Discounting Chain`, the first action (which is categorical) causes a reward that is only provided after a certain number of steps, specified by the parameter *reward delay*.

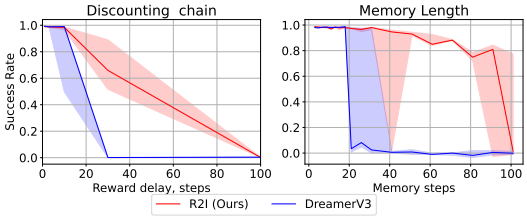

Figure 3: Success rates of DreamerV3 (which holds the previous SOTA) and R2I in BSuite environments. A separate model is trained for every point on the x-axis. A median value (over 10 seeds) is plotted filling between 25-th and 75-th percentiles. Training curves are in Appendix G.

As depicted in Figure 3, the previous SOTA DreamerV3 learns the dependencies between actions and rewards in both `Discounting Chain` and `Memory Length` with reward delays of up to 30 environment steps. Note that every run either converged to a maximum reward or failed (based on the random seed). We plot the success rate as the fraction of runs that achieved success. R2I excels in both tasks, significantly outperforming in the preservation of its learning ability across a wider range of varying environment complexities. In these experiments, we leverage the output state policy (i.e., operating on latent variable z_t and S3M output h_t). More details are provided in Appendix F.

POPGym experiments. We perform a study to assess R2I in a more challenging benchmark, namely, POPGym (Morad et al., 2023). This suite offers a range of RL environments designed to assess various challenges related to POMDPs, such as navigation, noise robustness, and memory. Based on Ni et al. (2023), we select the three most memory-intensive environments: `RepeatPrevious`, `Autoencode`, and `Concentration`. These environments require an optimal policy to memorize the highest number of events (i.e., actions or observations) at each time step. Each environment in POPGym has three difficulty levels: `Easy`, `Medium`, and `Hard`. In the memory environments of this study, the complexity is increased by the number of actions or observations that the agent should keep track of *simultaneously*. All environments in this study have categorical observation and action spaces. A detailed explanation of the environments is provided in Appendix H.

	`RepeatPrev.`			`Autoenc.`			`Conc.`		
	`-E`	`-M`	`-H`	`-E`	`-M`	`-H`	`-E`	`-M`	`-H`
Parallel events	4	32	64	52	104	156	104	208	104
$\lvert\mathcal{O}\rvert$		4			4		3	3	14
Memory-less suboptimal[1]		✗			✗			✓	

Table 2: Memory complexities of environments in POPgym. "Parallel events" refers to the maximum number of actions or observations that the agent needs to remember. $|\mathcal{O}|$ is the size of the observation space. The third row indicates whether the task can be partially solved without memory. `-E` is `-Easy`; `-M` is `-Medium`; `-H` is `-Hard`.

As POPGym was not included in the DreamerV3 benchmark, we performed hyperparameter tuning of both DreamerV3 and R2I, solely on adjusting the network sizes of both. This is because DreamerV3 is a generalist agent that works with a fixed set of hyperparameters and in this environment, with sizes primarily influencing its data efficiency. We observed a similar characteristic in R2I. The results of hyperparameter tuning are available in Appendix M. For R2I, we use the hidden state policy: $\pi(\hat{a}_t \mid z_t, h_t)$ as we found it much more performant, especially in memory-intensive tasks (see Appendix O for policy inputs ablations). We train R2I in POPGym environments using a unified and fixed set of hyperparameters. In addition to R2I and DreamerV3, we include model-free baselines from Morad et al. (2023). These include PPO (Schulman et al., 2017) model-free policy with different observation backbones, such as GRU, LSTM, MLP, and MLP with timestep number added as a

[1] A policy without any memory exists that outperforms a random policy but underperforms the optimal one.

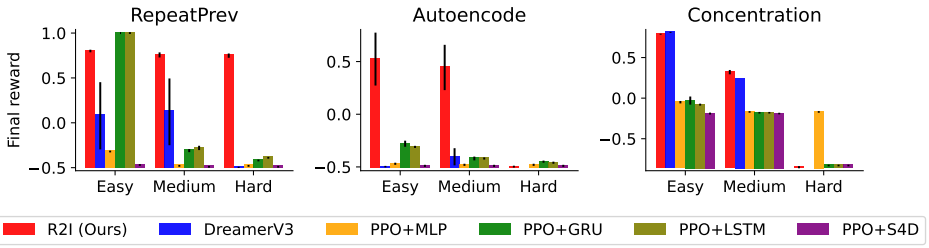

Figure 4: R2I results in memory-intensive environments of POPGym. Our method establishes the new SOTA in the hardest memory environments; `Autoencode`: `-Easy`, `-Medium`; `RepeatPrevious`: `-Medium`, `-Hard`; `Concentration`: `-Medium`. Note that `Concentration` is a task that can be partially solved without memory. For `PPO+S4D`, refer to T

feature (PosMLP). PPO with GRU is the best-performing model-free baseline of POPGym while PPO+LSTM is the second best. PPO+MLP and PPO+PosMLP are included for a sanity check - the better their performance is, the less is the memory needed in the environment

As illustrated in Figure 4, R2I demonstrates the new SOTA performance, outperforming every baseline in `Autoencode`, `Easy` and `Medium` tasks. Note that R2I outperforms all 13 model-free baselines of the POPGym benchmark by a huge margin (we did not include them due to space constraints). R2I also shows consistently strong performance in `RepeatPrevious` tasks, setting a new SOTA in both `Medium` and `Hard` (compared to all 13 model-free baselines and DreamerV3). In `Concentration`, the model-free memory baselines fail to outperform a simple MLP policy, suggesting that they all converge to a non-memory-based suboptimal policy. R2I advances this towards a better memory policy. Its performance is roughly equal to DreamerV3 in an `Easy` and slightly better in the `Medium` task. As the Table 2 suggests, all `RepeatPrevious` tasks require up to 64 memorization steps, while `Autoencode Easy` and `Medium` require up to 104. In `Concentration Easy` and `Medium` this length is up to 208 steps, however, since PPO+MLP shows somewhat good performance, likely less than 208 memorization steps are required. This observation is consistent with the results of the BSuite experiments, which demonstrate that our model is capable of memorizing up to approximately 100 steps in time. To summarize, **these results indicate that R2I significantly pushes the memory limits**.

4.2 Evaluating Long-term Memory In Complex 3D Tasks

Memory Maze (Pasukonis et al., 2022) presents randomized 3D mazes where the egocentric agent is repeatedly tasked to navigate to one of multiple objects. For optimal speed and efficiency, the agent must retain information about the locations of objects, the maze's wall layout, and its own position. Each episode can extend for up to 4K environment steps. An ideal agent equipped with long-term memory only needs to explore each maze once, a task achievable in a shorter time than the episode's duration; subsequently, it can efficiently find the shortest path to reach each requested target. This task poses a fundamental challenge for existing memory-augmented RL algorithms, which fall significantly behind human performance in these tasks.

In this benchmark, we found that DreamerV3 works equally well as DreamerV2 reported in Pasukonis et al. (2022). Therefore, we use the size configuration of Dreamer outlined in Pasukonis et al. (2022). Note that this baseline also leverages truncated backpropagation through time (TBTT), a technique demonstrated to enhance the preservation of information over time (Pasukonis et al., 2022). We use the "medium memory" size configuration of R2I in this work (see Table 3 in Appendix). We use the full state policy ($\pi(\hat{a}_t \mid z_t, h_t, x_t)$ i.e., conditioning on stochastic state, and S3M output, and hidden states at step t) in this environment. We trained and tested R2I and other methods on 4 existing maze sizes: 9x9, 11x11, 13x13, and 15x15. The difference between them is in the number of object rooms and the episode lengths. More difficult maze sizes have more environment steps in the episode making it more challenging to execute a successful series of object searches. R2I and other baselines are evaluated after 100M environment steps of training. We also compare R2I with IMPALA (Espeholt et al., 2018), which is the leading model-free approach (Pasukonis et al., 2022).

As shown in Figure 5, R2I consistently outperforms baseline methods in all of these environments, achieving comparable or higher levels of performance. In 9x9 mazes, it demonstrates performance

similar to the Dreamer, while significantly outperforming IMPALA. In 11x11 and 13x13 mazes, it has a remarkably better performance than both baselines. In 15x15 mazes, R2I outperforms Dreamer, while matching the performance of IMPALA. **These results establish R2I as a SOTA in this complex 3D domain**.

4.3 Assessing the Generality of R2I in Non-Memory Domains

We conduct a sanity check by assessing R2I's performance on two widely used RL benchmarks: Atari (Bellemare et al., 2013) and DMC (Tassa et al., 2018), as parts of the DreamerV3 benchmark (Hafner et al., 2023). Even though these tasks are nearly fully observable and do not necessitate extensive memory to solve (it is often enough to model the dynamics of only the last few steps), evaluating R2I on them is essential as we aim to ensure our agent's performance across a wide range of tasks that require different types of control: continuous control (in DMC) and discrete (in Atari).

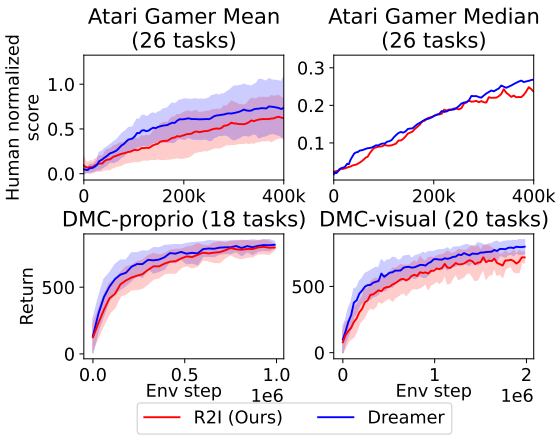

Figure 6: Average performance in Atari and DMC. For full training curves, see Appendix L (Atari), Appendix J (DMC-P), and Appendix K (DMC-V)

In all the experiments conducted within Atari 100K (Łukasz Kaiser et al., 2020) and DMC, we fix hyperparameters of the world model. In Atari and the proprio benchmark in DMC, we utilize output state policies, as we found them more performant (for ablations with different policy types, see Appendix O). In the visual benchmark in DMC, we use hidden state policy. Note that for continuous control, the policy is trained via differentiating through the learned dynamics. R2I maintains a performance similar to DreamerV3 in these domains, as demonstrated in Figure 6, implying that in the majority of standard RL tasks (see Appendix R), **R2I does not sacrifice generality for improved memory capabilities**.

5 Conclusion

In this paper, we introduced R2I, a general and fast model-based approach to reinforcement learning that demonstrates superior memory capabilities. R2I integrates two strong algorithms: DreamerV3, a general-purpose MBRL algorithm, and SSMs, a family of novel parallelizable sequence models adept at handling extremely long-range dependencies. This integration helps rapid long-term memory and long-horizon credit assignment, allowing R2I to excel across a diverse set of domains, all while maintaining fixed hyperparameters across all domains. Through a systematic examination, we have demonstrated that R2I sets a new state-of-the-art in domains demanding long-term temporal reasoning: it outperforms all known baselines by a large margin on the most challenging memory and credit assignment tasks across different types of memory (long-term and short-term) and observational complexities (tabular and complex 3D). Furthermore, we have demonstrated that R2I achieves computation speeds up to 9 times faster than DreamerV3.

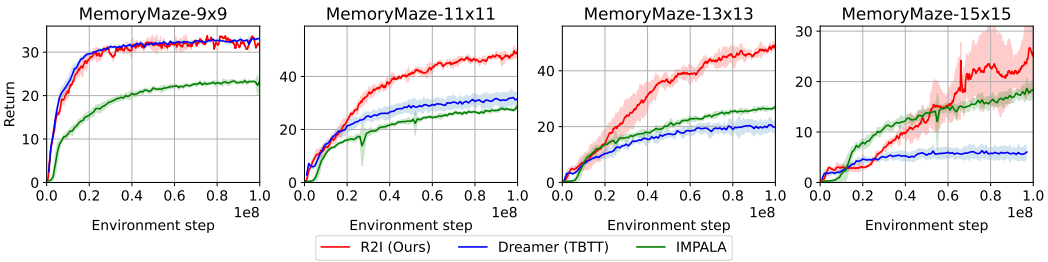

Figure 5: Scores in Memory Maze after 100M environment steps. R2I outperforms baselines across difficulty levels, becoming the domain's new SOTA.

Our study presents the first model-based RL approach that uses SSMs. Concurrently with this work, S4WM (Deng et al., 2023) has also explored the utilization of SSMs for enhancing world models within the context of SSL, a subtask in MBRL. As we discuss in Appendix Q, while improved world modeling is a valuable component, it alone does not guarantee enhanced performance in RL (Nikishin et al., 2021). While R2I offers benefits for improving memory in RL, it also has limitations, which we leave for future research. For instance, it can be explored how R2I can be augmented with attention mechanisms, given that Transformers and SSMs exhibit complementary strengths (Mehta et al., 2022). As mentioned in Section 2.1, hybrid architectures have been introduced in language modeling tasks. Moreover, the sequence length within the training batches for world model learning is not currently extremely long, as is the horizon (i.e., the number of steps) of imagination in actor-critic learning. Future work could focus on these aspects to further enhance memory capabilities.

6 ACKNOWLEDGEMENTS

We thank Albert Gu for his thorough and insightful feedback on the SSM part of the project. We also acknowledge The Annotated S4 Blog (Rush & Karamcheti, 2022) and S5 codebase (Smith et al., 2023) which inspired our JAX implementation. We also thank Danijar Hafner, Steven Morad, Ali Rahimi-Kalahroudi, Michel Ma, Tianwei Ni, Darshan Patil, Roger Creus for their helpful feedback on our method and on the early draft of the paper. We thank Jurgis Pasukonis for sharing the data for memory maze baseline plots. This research was enabled by compute resources provided by Mila (mila.quebec), the Digital Research Alliance of Canada (alliancecan.ca), and NVIDIA (nvidia.com). We thank Mila's IDT team, and especially Olexa Bilaniuk for helping with numerous technical questions during this work and especially for the help in the implementation of the new I/O efficient RL replay buffer. Janarthanan Rajendran acknowledges the support of the IVADO postdoctoral fellowship. Sarath Chandar is supported by the Canada CIFAR AI Chairs program, the Canada Research Chair in Lifelong Machine Learning, and the NSERC Discovery Grant.

REFERENCES

Gradient-based learning applied to document recognition. *Proceedings of the IEEE*, 86(11):2278–2324, 1998.

Mohammed Abbad. *Perturbation and stability theory for Markov control problems*. University of Maryland, Baltimore County, 1991.

Rishabh Agarwal, Max Schwarzer, Pablo Samuel Castro, Aaron Courville, and Marc G Bellemare. Deep reinforcement learning at the edge of the statistical precipice. *Advances in Neural Information Processing Systems*, 2021.

Jose A Arjona-Medina, Michael Gillhofer, Michael Widrich, Thomas Unterthiner, Johannes Brandstetter, and Sepp Hochreiter. Rudder: Return decomposition for delayed rewards. *Advances in Neural Information Processing Systems*, 32, 2019.

Jimmy Lei Ba, Jamie Ryan Kiros, and Geoffrey E. Hinton. Layer normalization, 2016.

M. G. Bellemare, Y. Naddaf, J. Veness, and M. Bowling. The arcade learning environment: An evaluation platform for general agents. *Journal of Artificial Intelligence Research*, 47:253–279, jun 2013. doi: 10.1613/jair.3912. URL https://doi.org/10.1613%2Fjair.3912.

Yoshua Bengio, Patrice Simard, and Paolo Frasconi. Learning long-term dependencies with gradient descent is difficult. *IEEE transactions on neural networks*, 5(2):157–166, 1994.

Guy E. Blelloch. Prefix sums and their applications. Technical Report CMU-CS-90-190, School of Computer Science, Carnegie Mellon University, November 1990.

William L Brogan. *Modern control theory*. Pearson education india, 1991.

Tom B. Brown, Benjamin Mann, Nick Ryder, Melanie Subbiah, Jared Kaplan, Prafulla Dhariwal, Arvind Neelakantan, Pranav Shyam, Girish Sastry, Amanda Askell, Sandhini Agarwal, Ariel Herbert-Voss, Gretchen Krueger, Tom Henighan, Rewon Child, Aditya Ramesh, Daniel M. Ziegler, Jeffrey Wu, Clemens Winter, Christopher Hesse, Mark Chen, Eric Sigler, Mateusz Litwin, Scott Gray, Benjamin Chess, Jack Clark, Christopher Berner, Sam McCandlish, Alec Radford, Ilya Sutskever, and Dario Amodei. Language models are few-shot learners, 2020.

Aydar Bulatov, Yuri Kuratov, and Mikhail S. Burtsev. Recurrent memory transformer, 2022.

Chang Chen, Yi-Fu Wu, Jaesik Yoon, and Sungjin Ahn. Transdreamer: Reinforcement learning with transformer world models, 2022.

Kyunghyun Cho, Bart van Merrienboer, Caglar Gulcehre, Dzmitry Bahdanau, Fethi Bougares, Holger Schwenk, and Yoshua Bengio. Learning phrase representations using rnn encoder-decoder for statistical machine translation, 2014.

Krzysztof Choromanski, Valerii Likhosherstov, David Dohan, Xingyou Song, Andreea Gane, Tamas Sarlos, Peter Hawkins, Jared Davis, Afroz Mohiuddin, Lukasz Kaiser, David Belanger, Lucy Colwell, and Adrian Weller. Rethinking attention with performers, 2022.

Zihang Dai, Zhilin Yang, Yiming Yang, Jaime Carbonell, Quoc V. Le, and Ruslan Salakhutdinov. Transformer-xl: Attentive language models beyond a fixed-length context, 2019.

Tri Dao, Daniel Y. Fu, Stefano Ermon, Atri Rudra, and Christopher Ré. Flashattention: Fast and memory-efficient exact attention with io-awareness, 2022.

Yann N. Dauphin, Angela Fan, Michael Auli, and David Grangier. Language modeling with gated convolutional networks. In Doina Precup and Yee Whye Teh (eds.), *Proceedings of the 34th International Conference on Machine Learning*, volume 70 of *Proceedings of Machine Learning Research*, pp. 933–941. PMLR, 06–11 Aug 2017. URL https://proceedings.mlr.press/v70/dauphin17a.html.

Shmuel Bar David, Itamar Zimerman, Eliya Nachmani, and Lior Wolf. Decision s4: Efficient sequence-based RL via state spaces layers. In *The Eleventh International Conference on Learning Representations*, 2023. URL https://openreview.net/forum?id=kqHkCVS7wbj.

Fei Deng, Junyeong Park, and Sungjin Ahn. Facing off world model backbones: Rnns, transformers, and s4, 2023.

Jiayu Ding, Shuming Ma, Li Dong, Xingxing Zhang, Shaohan Huang, Wenhui Wang, Nanning Zheng, and Furu Wei. Longnet: Scaling transformers to 1,000,000,000 tokens, 2023.

Lasse Espeholt, Hubert Soyer, Remi Munos, Karen Simonyan, Volodymir Mnih, Tom Ward, Yotam Doron, Vlad Firoiu, Tim Harley, Iain Dunning, Shane Legg, and Koray Kavukcuoglu. Impala: Scalable distributed deep-rl with importance weighted actor-learner architectures, 2018.

Kevin Esslinger, Robert Platt, and Christopher Amato. Deep transformer q-networks for partially observable reinforcement learning. *arXiv preprint arXiv:2206.01078*, 2022.

Mahan Fathi, Jonathan Pilault, Pierre-Luc Bacon, Christopher Pal, Orhan Firat, and Ross Goroshin. Block-state transformer, 2023.

Daniel Y. Fu, Tri Dao, Khaled K. Saab, Armin W. Thomas, Atri Rudra, and Christopher Ré. Hungry hungry hippos: Towards language modeling with state space models, 2023.

Albert Gu, Tri Dao, Stefano Ermon, Atri Rudra, and Christopher Ré. Hippo: Recurrent memory with optimal polynomial projections. *Advances in neural information processing systems*, 33: 1474–1487, 2020.

Albert Gu, Karan Goel, and Christopher Ré. Efficiently modeling long sequences with structured state spaces. *arXiv preprint arXiv:2111.00396*, 2021a.

Albert Gu, Isys Johnson, Karan Goel, Khaled Saab, Tri Dao, Atri Rudra, and Christopher Ré. Combining recurrent, convolutional, and continuous-time models with linear state-space layers. *Advances in Neural Information Processing Systems*, 34, 2021b.

Albert Gu, Ankit Gupta, Karan Goel, and Christopher Ré. On the parameterization and initialization of diagonal state space models, 2022.

Ankit Gupta, Albert Gu, and Jonathan Berant. Diagonal state spaces are as effective as structured state spaces, 2022a.

Ankit Gupta, Harsh Mehta, and Jonathan Berant. Simplifying and understanding state space models with diagonal linear rnns, 2022b.

David Ha and Jürgen Schmidhuber. World models. 2018. doi: 10.5281/ZENODO.1207631. URL `https://zenodo.org/record/1207631`.

Danijar Hafner, Timothy Lillicrap, Jimmy Ba, and Mohammad Norouzi. Dream to control: Learning behaviors by latent imagination. *arXiv preprint arXiv:1912.01603*, 2019a.

Danijar Hafner, Timothy Lillicrap, Ian Fischer, Ruben Villegas, David Ha, Honglak Lee, and James Davidson. Learning latent dynamics for planning from pixels. In *International Conference on Machine Learning*, pp. 2555–2565, 2019b.

Danijar Hafner, Timothy Lillicrap, Mohammad Norouzi, and Jimmy Ba. Mastering atari with discrete world models. *arXiv preprint arXiv:2010.02193*, 2020.

Danijar Hafner, Jurgis Pasukonis, Jimmy Ba, and Timothy Lillicrap. Mastering diverse domains through world models. *arXiv preprint arXiv:2301.04104*, 2023.

Dan Hendrycks and Kevin Gimpel. Gaussian error linear units (gelus), 2023.

Irina Higgins, Loic Matthey, Arka Pal, Christopher Burgess, Xavier Glorot, Matthew Botvinick, Shakir Mohamed, and Alexander Lerchner. beta-VAE: Learning basic visual concepts with a constrained variational framework. In *International Conference on Learning Representations*, 2017. URL `https://openreview.net/forum?id=Sy2fzU9gl`.

Sepp Hochreiter and Jürgen Schmidhuber. Long short-term memory. *Neural computation*, 9(8): 1735–1780, 1997.

Chia-Chun Hung, Timothy Lillicrap, Josh Abramson, Yan Wu, Mehdi Mirza, Federico Carnevale, Arun Ahuja, and Greg Wayne. Optimizing agent behavior over long time scales by transporting value. *Nature communications*, 10(1):5223, 2019.

Joshua Joseph, Alborz Geramifard, John W Roberts, Jonathan P How, and Nicholas Roy. Reinforcement learning with misspecified model classes. In *2013 IEEE International Conference on Robotics and Automation*, pp. 939–946. IEEE, 2013.

Gabriel Kalweit and Joschka Boedecker. Uncertainty-driven imagination for continuous deep reinforcement learning. In Sergey Levine, Vincent Vanhoucke, and Ken Goldberg (eds.), *Proceedings of the 1st Annual Conference on Robot Learning*, volume 78 of *Proceedings of Machine Learning Research*, pp. 195–206. PMLR, 13–15 Nov 2017. URL https://proceedings.mlr.press/v78/kalweit17a.html.

Steven Kapturowski, Georg Ostrovski, Will Dabney, John Quan, and Remi Munos. Recurrent experience replay in distributed reinforcement learning. In *International Conference on Learning Representations*, 2019. URL https://openreview.net/forum?id=r1lyTjAqYX.

Alex Krizhevsky, Geoffrey Hinton, et al. Learning multiple layers of features from tiny images. 2009.

Nathan Lambert, Brandon Amos, Omry Yadan, and Roberto Calandra. Objective mismatch in model-based reinforcement learning. *arXiv preprint arXiv:2002.04523*, 2020.

Chris Lu, Yannick Schroecker, Albert Gu, Emilio Parisotto, Jakob Foerster, Satinder Singh, and Feryal Behbahani. Structured state space models for in-context reinforcement learning, 2023.

Xuezhe Ma, Chunting Zhou, Xiang Kong, Junxian He, Liangke Gui, Graham Neubig, Jonathan May, and Luke Zettlemoyer. Mega: Moving average equipped gated attention, 2023.

Harsh Mehta, Ankit Gupta, Ashok Cutkosky, and Behnam Neyshabur. Long range language modeling via gated state spaces. *arXiv preprint arXiv:2206.13947*, 2022.

Stephen Merity, Caiming Xiong, James Bradbury, and Richard Socher. Pointer sentinel mixture models, 2016.

Vincent Micheli, Eloi Alonso, and François Fleuret. Transformers are sample-efficient world models, 2023.

Thomas M. Moerland, Joost Broekens, Aske Plaat, and Catholijn M. Jonker. Model-based reinforcement learning: A survey, 2022.

Steven Morad, Ryan Kortvelesy, Matteo Bettini, Stephan Liwicki, and Amanda Prorok. POPGym: Benchmarking partially observable reinforcement learning. In *The Eleventh International Conference on Learning Representations*, 2023. URL https://openreview.net/forum?id=chDrutUTs0K.

Eric Nguyen, Karan Goel, Albert Gu, Gordon Downs, Preey Shah, Tri Dao, Stephen Baccus, and Christopher Ré. S4nd: Modeling images and videos as multidimensional signals with state spaces. *Advances in neural information processing systems*, 35:2846–2861, 2022.

Tianwei Ni, Michel Ma, Benjamin Eysenbach, and Pierre-Luc Bacon. When do transformers shine in rl? decoupling memory from credit assignment, 2023.

Evgenii Nikishin, Romina Abachi, Rishabh Agarwal, and Pierre-Luc Bacon. Control-oriented model-based reinforcement learning with implicit differentiation, 2021.

Ian Osband, Yotam Doron, Matteo Hessel, John Aslanides, Eren Sezener, Andre Saraiva, Katrina McKinney, Tor Lattimore, Csaba Szepesvári, Satinder Singh, Benjamin Van Roy, Richard Sutton, David Silver, and Hado van Hasselt. Behaviour suite for reinforcement learning. In *International Conference on Learning Representations*, 2020. URL https://openreview.net/forum?id=rygf-kSYwH.

Emilio Parisotto, Francis Song, Jack Rae, Razvan Pascanu, Caglar Gulcehre, Siddhant Jayakumar, Max Jaderberg, Raphael Lopez Kaufman, Aidan Clark, Seb Noury, et al. Stabilizing transformers for reinforcement learning. In *International conference on machine learning*, pp. 7487–7498. PMLR, 2020.

Razvan Pascanu, Tomas Mikolov, and Yoshua Bengio. On the difficulty of training recurrent neural networks, 2013.

Jurgis Pasukonis, Timothy Lillicrap, and Danijar Hafner. Evaluating long-term memory in 3d mazes. *arXiv preprint arXiv:2210.13383*, 2022.

David Raposo, Sam Ritter, Adam Santoro, Greg Wayne, Theophane Weber, Matt Botvinick, Hado van Hasselt, and Francis Song. Synthetic returns for long-term credit assignment. *arXiv preprint arXiv:2102.12425*, 2021.

Jan Robine, Marc Höftmann, Tobias Uelwer, and Stefan Harmeling. Transformer-based world models are happy with 100k interactions. In *The Eleventh International Conference on Learning Representations*, 2023. URL https://openreview.net/forum?id=TdBaDGCpjly.

Alexander Rush and Sidd Karamcheti. The annotated s4. In *ICLR Blog Track*, 2022. URL https://iclr-blog-track.github.io/2022/03/25/annotated-s4/. https://iclr-blog-track.github.io/2022/03/25/annotated-s4/.

Julian Schrittwieser, Ioannis Antonoglou, Thomas Hubert, Karen Simonyan, Laurent Sifre, Simon Schmitt, Arthur Guez, Edward Lockhart, Demis Hassabis, Thore Graepel, Timothy Lillicrap, and David Silver. Mastering atari, go, chess and shogi by planning with a learned model. *Nature*, 588 (7839):604–609, dec 2020. doi: 10.1038/s41586-020-03051-4. URL https://doi.org/10.1038%2Fs41586-020-03051-4.

John Schulman, Filip Wolski, Prafulla Dhariwal, Alec Radford, and Oleg Klimov. Proximal policy optimization algorithms, 2017.

Burrhus Frederic Skinner. *The behavior of organisms: An experimental analysis*. BF Skinner Foundation, 2019.

Jimmy T. H. Smith, Andrew Warrington, and Scott W. Linderman. Simplified state space layers for sequence modeling, 2023.

Richard S Sutton. Integrated architectures for learning, planning, and reacting based on approximating dynamic programming. In *Machine learning proceedings 1990*, pp. 216–224. Elsevier, 1990.

Yuval Tassa, Yotam Doron, Alistair Muldal, Tom Erez, Yazhe Li, Diego de Las Casas, David Budden, Abbas Abdolmaleki, Josh Merel, Andrew Lefrancq, Timothy Lillicrap, and Martin Riedmiller. Deepmind control suite, 2018.

Yi Tay, Mostafa Dehghani, Samira Abnar, Yikang Shen, Dara Bahri, Philip Pham, Jinfeng Rao, Liu Yang, Sebastian Ruder, and Donald Metzler. Long range arena: A benchmark for efficient transformers, 2020.

Yi Tay, Mostafa Dehghani, Samira Abnar, Yikang Shen, Dara Bahri, Philip Pham, Jinfeng Rao, Liu Yang, Sebastian Ruder, and Donald Metzler. Long range arena : A benchmark for efficient transformers. In *International Conference on Learning Representations*, 2021. URL https://openreview.net/forum?id=qVyeW-grC2k.

Romal Thoppilan, Daniel De Freitas, Jamie Hall, Noam Shazeer, Apoorv Kulshreshtha, Heng-Tze Cheng, Alicia Jin, Taylor Bos, Leslie Baker, Yu Du, YaGuang Li, Hongrae Lee, Huaixiu Steven Zheng, Amin Ghafouri, Marcelo Menegali, Yanping Huang, Maxim Krikun, Dmitry Lepikhin, James Qin, Dehao Chen, Yuanzhong Xu, Zhifeng Chen, Adam Roberts, Maarten Bosma, Vincent Zhao, Yanqi Zhou, Chung-Ching Chang, Igor Krivokon, Will Rusch, Marc Pickett, Pranesh Srinivasan, Laichee Man, Kathleen Meier-Hellstern, Meredith Ringel Morris, Tulsee Doshi, Renelito Delos Santos, Toju Duke, Johnny Soraker, Ben Zevenbergen, Vinodkumar Prabhakaran, Mark Diaz, Ben Hutchinson, Kristen Olson, Alejandra Molina, Erin Hoffman-John, Josh Lee, Lora Aroyo, Ravi Rajakumar, Alena Butryna, Matthew Lamm, Viktoriya Kuzmina, Joe Fenton, Aaron Cohen, Rachel Bernstein, Ray Kurzweil, Blaise Aguera-Arcas, Claire Cui, Marian Croak, Ed Chi, and Quoc Le. Lamda: Language models for dialog applications, 2022.

Ashish Vaswani, Noam Shazeer, Niki Parmar, Jakob Uszkoreit, Llion Jones, Aidan N Gomez, Łukasz Kaiser, and Illia Polosukhin. Attention is all you need. *Advances in neural information processing systems*, 30, 2017.

Andreas Veit, Michael Wilber, and Serge Belongie. Residual networks behave like ensembles of relatively shallow networks, 2016.

Junxiong Wang, Jing Nathan Yan, Albert Gu, and Alexander M. Rush. Pretraining without attention, 2023.

Qiang Wang, Bei Li, Tong Xiao, Jingbo Zhu, Changliang Li, Derek F. Wong, and Lidia S. Chao. Learning deep transformer models for machine translation. In Anna Korhonen, David Traum, and Lluís Màrquez (eds.), *Proceedings of the 57th Annual Meeting of the Association for Computational Linguistics*, pp. 1810–1822, Florence, Italy, July 2019. Association for Computational Linguistics. doi: 10.18653/v1/P19-1176. URL https://aclanthology.org/P19-1176.

Sinong Wang, Belinda Z. Li, Madian Khabsa, Han Fang, and Hao Ma. Linformer: Self-attention with linear complexity, 2020.

Pete Warden. Speech commands: A dataset for limited-vocabulary speech recognition, 2018.

Michael Widrich, Markus Hofmarcher, Vihang Prakash Patil, Angela Bitto-Nemling, and Sepp Hochreiter. Modern hopfield networks for return decomposition for delayed rewards. In *Deep RL Workshop NeurIPS 2021*, 2021.

Ronald J. Williams. Simple statistical gradient-following algorithms for connectionist reinforcement learning. *Mach. Learn.*, 8(3–4):229–256, may 1992. ISSN 0885-6125. doi: 10.1007/BF00992696. URL https://doi.org/10.1007/BF00992696.

Weirui Ye, Shaohuai Liu, Thanard Kurutach, Pieter Abbeel, and Yang Gao. Mastering atari games with limited data, 2021.

Manzil Zaheer, Guru Guruganesh, Avinava Dubey, Joshua Ainslie, Chris Alberti, Santiago Ontanon, Philip Pham, Anirudh Ravula, Qifan Wang, Li Yang, and Amr Ahmed. Big bird: Transformers for longer sequences, 2021.

Susan Zhang, Stephen Roller, Naman Goyal, Mikel Artetxe, Moya Chen, Shuohui Chen, Christopher Dewan, Mona Diab, Xian Li, Xi Victoria Lin, Todor Mihaylov, Myle Ott, Sam Shleifer, Kurt Shuster, Daniel Simig, Punit Singh Koura, Anjali Sridhar, Tianlu Wang, and Luke Zettlemoyer. Opt: Open pre-trained transformer language models, 2022.

Simiao Zuo, Xiaodong Liu, Jian Jiao, Denis Charles, Eren Manavoglu, Tuo Zhao, and Jianfeng Gao. Efficient long sequence modeling via state space augmented transformer. *arXiv preprint arXiv:2212.08136*, 2022.

Łukasz Kaiser, Mohammad Babaeizadeh, Piotr Miłos, Błażej Osiński, Roy H Campbell, Konrad Czechowski, Dumitru Erhan, Chelsea Finn, Piotr Kozakowski, Sergey Levine, Afroz Mohiuddin, Ryan Sepassi, George Tucker, and Henryk Michalewski. Model based reinforcement learning for atari. In *International Conference on Learning Representations*, 2020. URL https://openreview.net/forum?id=S1xCPJHtDB.

Appendix

Table of Contents

A FAQ

1. **Q: Why do you report the low performance of DreamerV3 on the BSuite `Memory Length` environment, whereas DreamerV3 reports a state-of-the-art score there?**

   DreamerV3 reports the score of 0.478 in the memory length environment of BSuite (see Table L.1 in Hafner et al. (2023)). This score is normalized to be in the range $[0, 1]$ and the score is formed by averaging many runs with different complexities (the episode length plays the role of complexity since the agent is tasked to remember the first observation throughout the whole episode). This can mean that it masters approximately half of the complexity values (because as Skinner (2019) reports, performance typically decreases monotonically as the complexity increases). At the same time, the complexities of this environment (i.e. episode lengths) fill the range $[1..100]$ logarithmically (see Appendix A.6.1 in Skinner (2019)). The episode length of 30 steps is approximately in the middle of the complexity range. In our experiments, we observed that the performance of DreamerV3 also decreases monotonically and it drops at approximately 30 steps, which is half of the tasks in memory length environment. Therefore, our result aligns with DreamerV3.

2. **Q: Why do you not perform architecturally fair experiments to compare DreamerV3 and R2I? For instance, you could make a potentially more powerful sequence block for a fair comparison by incorporating elements such as GLU, LayerNorm, skip connections, and dropout to the GRU cell in the Dreamer's world model.**

   The goal of our study was not to perform an apples-to-apples comparison across recurrent models in MBRL. Instead, we focused on building a black-box model that performs effectively across various environments and can efficiently scale with sequence length in batches (both in terms of being able to technically train on that batch and perform better with a varied length). This scaling would not be possible with standard RNNs due to the inability to execute parallel computations. While it may be feasible with Transformers, our argument suggests that they might not excel in specific memory-intensive tasks, such as when the information needed to predict a reward differs from that required to execute the optimal action.

3. **Q: Which type of SSMs do you use in R2I: S4, S5, S4D, S4ND, or another variant?**

   In Appendix C, we delve into various types of variations among SSMs. Some of these combinations of hyperparameters have established names in the literature. The one we found to be optimal in our case is slightly different from those previously introduced. However, these differences are minor details, and the model closest to the SSMs we implement is S5 (Smith et al., 2023).

4. **Q: What is the difference between SSM, RSSM, and S3M?**

   There exists a notational clash between what is traditionally meant by SSM and by RSSM. This clash arises because SSMs represent a distinct branch of research that is completely independent of MBRL with Dreamer and RSSM. As a result, they have different meanings. SSM can be considered a counterpart to any standard RNN, while RSSM is a special RNN-based model explicitly designed for use in latent world models. On the other hand, S3M is a modification of the RSSM that employs SSMs to serve as its internal sequence models.

5. **Q: Do you claim to have fixed hyperparameters across all domains, even though some of them might vary, such as policy input features or network sizes?**

   We only claim that the hyperparameters of the world model are fixed. Nonetheless, the policy inputs (e.g. whether it is (z_t, h_t) or (z_t, x_t)) need to be tuned. This is because different environments assume different levels of partial observability, which affects the information in z_t, h_t, and x_t. Maintaining (z_t, h_t, x_t) in the policy all the time is not a remedy, as it impacts the training dynamics considerably, as observed in (Robine et al., 2023)) due to the instability of features and the fact that the policy size changes significantly.

   Please note that while working within a specific domain, we fix all hyperparameters for the training agent (i.e., world model, policy, and their optimizers).

   However, we change the world model "scales" to match the complexity of environments within each domain. This adaptation is necessary because we cover very diverse environments (e.g., symbolic environments with observation and action space sizes equal to 4, or 3D egocentric environments in textured mazes). Hence, making the world model's hyperparameters completely unified would be impractical.

B Related Work

Addressing sequential decision-making problems requires the incorporation of temporal reasoning. This necessitates a crucial element of intelligence - *memory* (Parisotto et al., 2020; Esslinger et al., 2022; Morad et al., 2023). Essentially, memory enables humans and machines to retain valuable information from past events, empowering us to make informed decisions at present. But it does not stop there; another vital aspect is the ability to gauge the effects and consequences of our past actions and choices on the feedback/outcome we receive now - be it success or failure. This process is termed *credit assignment* (Hung et al., 2019; Arjona-Medina et al., 2019; Widrich et al., 2021; Raposo et al., 2021). In their recent work, Ni et al. (2023) explore the relationship between these two concepts, examining their interplay. The process of learning which parts of history to remember is deeply connected to the prediction of future rewards. Simultaneously, mastering the skill of distributing current rewards to past actions inherently involves a memory component.

To improve temporal reasoning, we leverage model-based RL (Moerland et al., 2022). The essence of MBRL lies in its utilization of a world model (Kalweit & Boedecker, 2017; Ha & Schmidhuber, 2018; Hafner et al., 2019b). The world model is employed to plan a sequence of actions that maximize the task reward (Hafner et al., 2019a; 2020; 2023; Schrittwieser et al., 2020; Ye et al., 2021; Micheli et al., 2023). Our focus on MBRL stems from its potential in sample efficiency, reusability, transferability, and safer planning, along with the advantage of more controllable aspects due to its explicit supervised learning component (i.e., world modeling). Within the realm of MBRL methodologies, we decided to build upon the SOTA DreamerV3 framework (Hafner et al., 2023), which has proven capacities for generalization, sample efficiency, and scalability.

MBRL researchers commonly utilize RNNs (Ha & Schmidhuber, 2018; Hafner et al., 2019a; 2020; 2023) or Transformers (Chen et al., 2022; Micheli et al., 2023; Robine et al., 2023) as the backbone of their world models to integrate temporal reasoning into the agent. However, both of these approaches face limitations when it comes to modeling long-range dependencies, as stated earlier in Section 1. Recent research indicates that SSMs (Gu et al., 2021a;b; Gupta et al., 2022a; Gu et al., 2022; Mehta et al., 2022; Gupta et al., 2022b; Smith et al., 2023; Ma et al., 2023) can replace Transformers, capturing dependencies in very long sequences more efficiently (sub-quadratic complexity) and in parallel. Thus, they can be a good candidate for a backbone architecture of world models. In a concurrent work, Deng et al. (2023) propose S4WM world model which employs the S4 model as the recurrence in RSSM. Though S4WM is a valuable improvement in the task of world modeling, it does not propose any method for RL or MBRL, as outlined in Appendix Q.

C Variations of SSMs and Our Design Choices

Structured State Space Sequence model (S4; Gu et al. (2021a)) is built upon classical state space models, which are commonly used in control theory (Brogan, 1991). As mentioned in the Section 2.1, S4 is built upon three pivotal and independent pillars:

- **Parametrization of the structure**. A pivotal aspect is how we parameterize the matrices. S4 conjugates matrices into a diagonal plus low-rank (DPLR).
- **Dimensionality of the SSM**. S4 utilizes separate linear transformations for each input dimension, known as single-input single-output (SISO) SSMs.
- **Computational modeling**. The third axis revolves around how we model the computation process to parallelize. Gu et al. (2021a) model the computation as a global convolution.

Recent works have introduced certain modifications to S4, specifically targeting these pillars. Some research (Gupta et al., 2022a; Smith et al., 2023) demonstrate that employing a diagonal approximation for the HiPPO (Gu et al., 2020) yields comparable performance and thus represents the state matrices as diagonal, instead of DPLR.

Regarding the second axis, Smith et al. (2023) tensorize the 1-D operations into a multi-input multi-output (MIMO) SSM, facilitating a more direct and simplified implementation of SSMs. Furthermore, Smith et al. (2023) replace the global convolution operation with a parallel scan operation, thereby eliminating the complex computation involved in the convolution kernel.

The synergy between these axes of variations may significantly influence the agent's behavior and performance. In the following section, we will demonstrate our process for choosing each option and examine how each axis influences the performance. We further will provide more in-depth information regarding our choices for SSM hyperparameters.

C.1 Design Decisions for SSM

C.1.1 SSM Parametrization

While parameterizing the state matrix as a DPLR matrix could potentially offer a more expressive representation compared to a diagonal SSM, our decision was to diagonalize it. This decision was made to simplify control while maintaining high performance. Notably, the works of Gupta et al. (2022a) and Gu et al. (2022) demonstrate the feasibility of achieving S4's level of performance by employing a significantly simpler, fully diagonal parameterization for state spaces.

C.1.2 SSM Dimensionality

We decided to employ MIMO SSMs, a choice influenced by a convergence of factors. Firstly, by utilizing MIMO, the latent size can be substantially reduced, optimizing computational resources and accelerating processing. As a result, the implementation of efficient parallelization is facilitated.

Further, MIMO SSMs eliminate the need for mixing layers and offer the flexibility to accommodate diverse dynamics and couplings of input features within each layer. This stands in contrast to independent SISO SSMs, which process each channel of input features separately and then combine them using a mixing layer. Accordingly, the MIMO approach enables distinct processing tailored to individual input channels, leading to enhanced model adaptability and improved feature representation (Smith et al., 2023).

To validate the benefits of this decision, an ablation study was conducted. This comparative analysis showcases the differences between MIMO and SISO SSMs, empirically demonstrating the advantages of the MIMO.

D Managing Several Episodes in a Sampled Sequence

As mentioned in Section 3, handling episode boundaries in the sampled sequences necessitates the world model's capability to reset the hidden state. Given our utilization of parallel scan (Blelloch, 1990) for SSM computational modeling, it follows that adaptations to the binary operator in Smith et al. (2023) are essential. As a reminder, SSMs unroll a linear time-invariant dynamical system in the following form:

$$x_n = \bar{\mathbf{A}} x_{n-1} + \bar{\mathbf{B}} u_n, \quad y_n = \bar{\mathbf{C}} x_n + \bar{\mathbf{D}} u_n$$

Smith et al. (2023) employ parallel scans for the efficient computation of SSM states, denoted as x_n. Parallel scans leverage the property that "associative" operations can be computed in arbitrary order. When employing an associative binary operator denoted as $\bullet$ on a sequence of L elements $[e_1, e_2, \ldots, e_L]$, parallel scan yields $[e_1, (e_1 \bullet e_2(, \ldots, (e_1 \bullet e_2 \bullet \cdots \bullet e_L)]$. It is worth mentioning that, parallel scan can be computed with a complexity of $\mathcal{O}(\log L)$. In Smith et al. (2023), the elements e_i and the operator $\bullet$ are defined as follows:

$$e_n = (e_{n,0}, e_{n,1}) = (\bar{A}, \bar{\mathbf{B}} u_n), \quad e_i \bullet e_j = \big(e_{j,0} \times e_{i,0}, e_{j,0} \cdot e_{i,1} + e_{j,1}\big)$$

Here, $\times$ is the matrix-matrix product, and $\cdot$ is the matrix-vector product. To make resettable states, we need to incorporate the "done" flag while ensuring the preservation of the associative property. To do so, every element e_n is defined as follows:

$$e_n = (e_{n,0}, e_{n,1}, e_{n,2}) = (\bar{\mathbf{A}}, \bar{\mathbf{B}} u_n, d_n)$$

where d_n represents the done flag for the nth element. Now, we present the modified binary operator $\bullet$, defined as:

$$e_i \bullet e_j := \big((1 - d_i) \cdot e_{j,0} \times e_{i,0} + e_{i,2} \cdot e_{j,0}, (1 - d_i) e_{j,0} \cdot e_{i,1} + e_{j,1}, e_{i,2} e_{j,2}\big)$$

It is important to highlight this reparameterization of the operator defined in Lu et al. (2023), eliminates the need for if/else conditions. Thus, as discussed in Lu et al. (2023), the modified operator remains associative and retains the desirable properties we aimed to achieve.

Unlike Lu et al. (2023), we no longer assume a hidden state initialized to $x_0 = 0$; hence, a different initialization becomes necessary, specifically $e_0 = (\mathbf{I}, x_0, 0)$.

E TRAINING ACTOR-CRITIC

The policy and value functions are trained using latent imagination, regardless of their input features. This process aligns with the methodology outlined in Section 2.2. It begins with the generation of initial stochastic states $z_{1:T} \sim q_\theta(z_{1:T} \mid o_{1:T})$ and the computation of the sequence of deterministic hidden states $h_{1:T}, x_{1:T} = f_\phi((a_{1:T}, z_{1:T}), x_0)$ through a parallel scan operation. We reuse the previously computed values of $z_{1:T}$, $h_{1:T}$, and $x_{1:T}$ during training, which the parallel scan facilitates, thus eliminating the requirement for several burn-in steps before imagination.

Denoting $x_{j|t}$ as the state of x after j steps of imagination, given t context steps, we initialize with $x_{0|t} = x_t$, $h_{0|t} = h_t$, and $z_{0|t} = z_t$. We then compute the action $\hat{a}_{0|t} \sim \pi(\hat{a} \mid z_{0|t}, h_{0|t}, x_{0|t})$ and after $h_{1|t}, x_{1|t} = f_\phi((\hat{a}_{0|t}, z_{0|t}), x_{0|t})$; $\hat{z}_{1|t} \sim p_\theta(\hat{z} \mid h_{1|t})$. This process continues for H steps, during which we compute $\hat{a}_{1:H|t}, \hat{z}_{1:H|t}, h_{1:H|t}$, rewards and continue flags are computed via $\hat{r}_{1:H|t} \sim p(\hat{r} \mid \hat{z}_{1:H|t}, h_{1:H|t})$, $\hat{c}_{1:H|t} \sim p(\hat{c} \mid \hat{z}_{1:H|t}, h_{1:H|t})$, respectively. The ultimate goal is to train the policy to maximize the estimated return that follows:

$$R^\lambda_{j|t} = \hat{r}_{j|t} + c_{j|t}\left((1-\lambda)v(\hat{z}_{j|t}, h_{j|t}, x_{j|t}) + \lambda R^\lambda_{j+1|t}\right), \quad R^\lambda_{H|t} = v(\hat{z}_{j|t}, h_{j|t}, x_{T|t}) \tag{8}$$

To train the actor and critic, we employ Reinforce (Williams, 1992) for scenarios with discrete action spaces, coupled with the method of backpropagation through latent dynamics as introduced by Hafner et al. (2020). Our approach adheres to the DreamerV3 protocol of training the actor and critic networks (Hafner et al., 2023), which includes utilization of the fixed entropy bonus, the use of twohot regression in critic, and the employment of percentile-based normalization for the returns.

F ALGORITHM HYPERPARAMETERS

	Small Memory	Small	Medium Memory
Used in	BSuite and POPgym	Atari and DMC	Memory Maze
h_t size	512	512	2048
x_t size, per layer	512	192	512
SSM layers	3	5	5
SSM units	1024	512	1024

Table 3: S3M size configurations used in This work

Name	**Value**
FIFO replay buffer size	10^7
Batch length, L	Length of Episode
Number of environment steps in batch[2]	4096
Nonlinearity	LayerNorm + SiLU
SSM discretization method	bilinear
SSM nonlinearity	GeLU + GLU + LayerNorm
SSM matrices parameterization	Diagonal
SSM dimensionality parameterization	MIMO
SSM matrix blocks number (HiPPOs number)	8
SSM discretization range	$(10^{-3}, 10^{-1})$
Latent variable	Multi-categorical
Categorical latent variable numer	32
Categorical classes number	32
Unimix probability	0.01
Learning rate	10^{-4}
Reconstruction loss weight, β_{pred}	1
Dynamics loss weight, β_{pred}	0.5
Representation loss weight, β_{rep}	0.1
World Model gradient clipping	1000
Adam epsilon	10^{-8}
Actor Critic Hyperparameters	
Imagination horizon	15
Discount γ	0.997
Return λ	0.95
Entropy weight	$3 \cdot 10^{-4}$
Critic EMA decay	0.98
Critic EMA regularizer	1
Return normalization scale	$\text{Per}(R, 95) - \text{Per}(R, 5)$
Return normalization decay	0.99
Adam epsilon	10^{-5}
Actor-Critic gradient clipping	100

Table 4: R2I hyperparameters. For a detailed description, follow Section 3 and Hafner et al. (2023).

[2]batch size is calculated accordingly

G BSUITE TRAINING CURVES

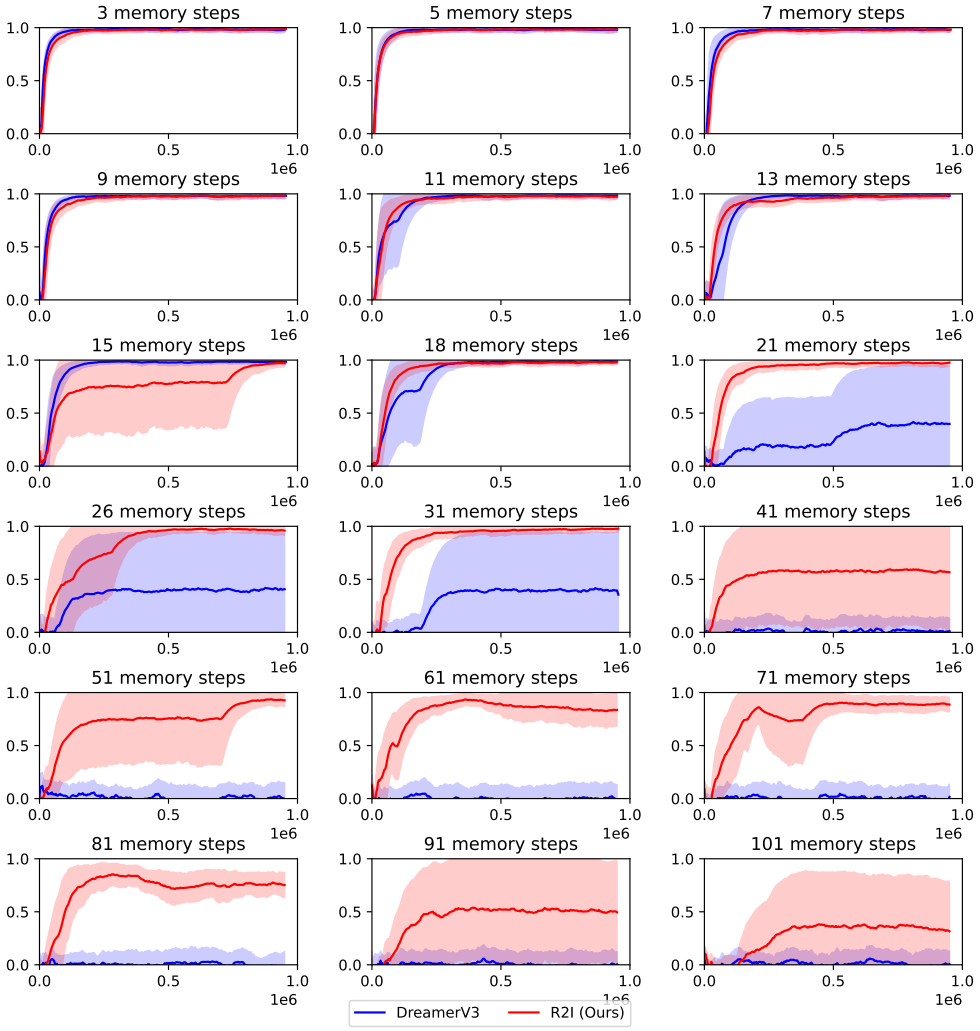

Figure 7: BSuite memory length training curves. 10 seeds per run. Median reward plotted.

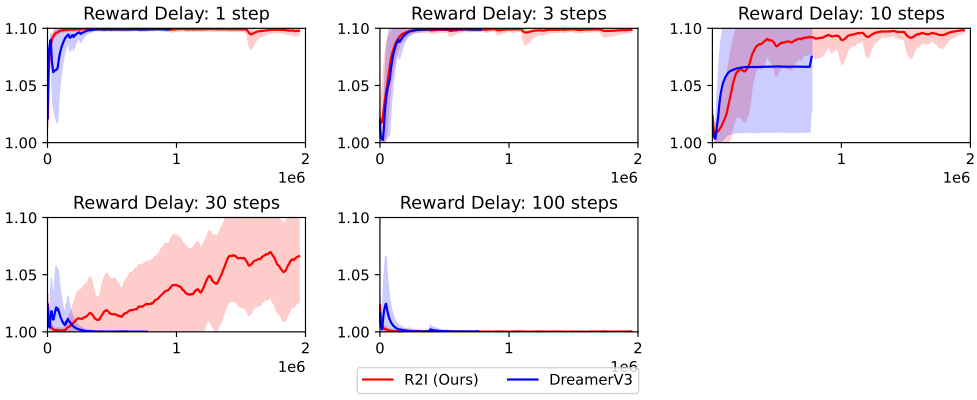

Figure 8: BSuite discounting chain training curves. 10 seeds per run. Median reward plotted.

H POPGYM ENVIRONMENTS DETAILS

In this research, we examine three environments from POPGym (Morad et al., 2023), each of which offers three difficulty levels: `Easy`, `Medium`, and `Hard`. Specifically for memory-intensive environments, the primary distinction across these difficulty tiers lies in the number of observations or actions agents need to memorize and recall, with more demanding memory assigned to the higher difficulty levels.

- `Autoencode`. The environment has two phases. During the first phase (which is called the "watch" phase), the environment generates an observation at each time step, with the observation space being discretely categorical, consisting of 4 values. Agent actions are not taken into account during the first phase. The "watch" phase lasts for $T/2$ steps, where T denotes the total length of the episode, which is set at 104 for `Easy`, 208 for `Medium`, and 312 for `Hard`. Once the "watch" phase ends the agent then enters the second phase. Here, the agent is expected to output each action (action space is equal to the observation space) equal to a corresponding observation from the first phase. In essence, the first action in phase two should match the first observation from phase one, the second action in phase two should correspond to the second observation from phase one, and so on. A phase flag, included in the agent's observation along with the categorical ID to be repeated, indicates the current phase. At each time step, the agent must remember $T/2$ categorical values. This task cannot be solved without explicit memory; therefore, any policy performing better than random chance is utilizing some form of memory.
- `RepeatPrevious`. This environment features simple categorical observation and action spaces (of the same size – 4). And the task is simply to output at step $t + k$ the action $a_{t+k} = o_t$, that is, repeat an observation that was exactly k steps ago. The agent at each time step needs to simultaneously remember k categorical values. For every difficulty, the size of the observation space is 4 and k is 4 for `Easy`, 32 for `Medium`, and 64 for `Hard`.
- `Concentration`. Each time step the agent receives a multi-categorical observation with 52 categories (for `Easy` and `Hard`) or 104 categories (for `Medium`). Each categorical has N values (3 for `Easy` and `Medium` and 14 for `Hard`). The environment represents a card game where all cards on a deck are spread face down (i.e. hidden). In each step, the agent flips a pair of cards and observes their values (the action space is the size of the deck). If the values are the same, the pair remains unflipped until the end of the game. Otherwise, they are flipped face down again. At each step, the agent receives the full deck as the observation. The episode length is equal to a theoretically minimal average number of steps that are required to solve a task (Morad et al., 2023). The optimal memory policy should memorize the card values if they don't match and then use that information to find matches faster. Even a memory-less policy can improve performance over the baseline by e.g. not trying to flip already "opened" cards (which has no effect in this game), thus not winning anything (i.e. not gaining new information and not getting a positive reward but wasting one time step). This is a minimal but most obvious improvement that a memory-less policy can gain over a random policy, though more advanced memory-less policies exist (Morad et al., 2023). Note that it has been proven this task cannot be solved without memory (due to the episode length constraint) (Morad et al., 2023).

I POPGym Training Curves

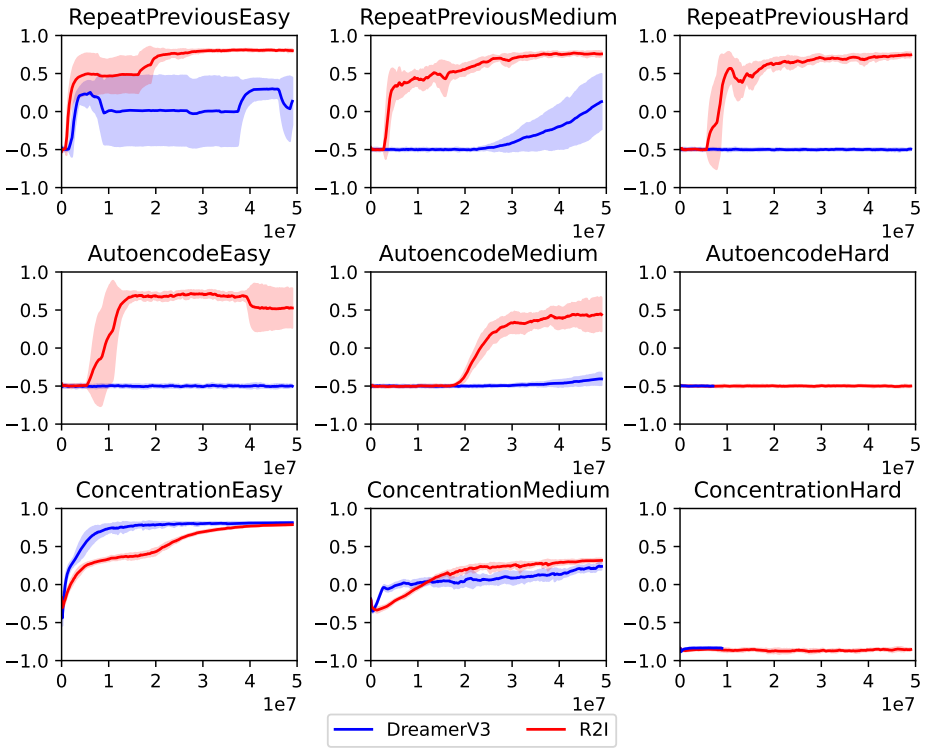

Figure 9: POPGym training curves. 3 seeds per run.

J DMC-PROPRIO TRAINING CURVES

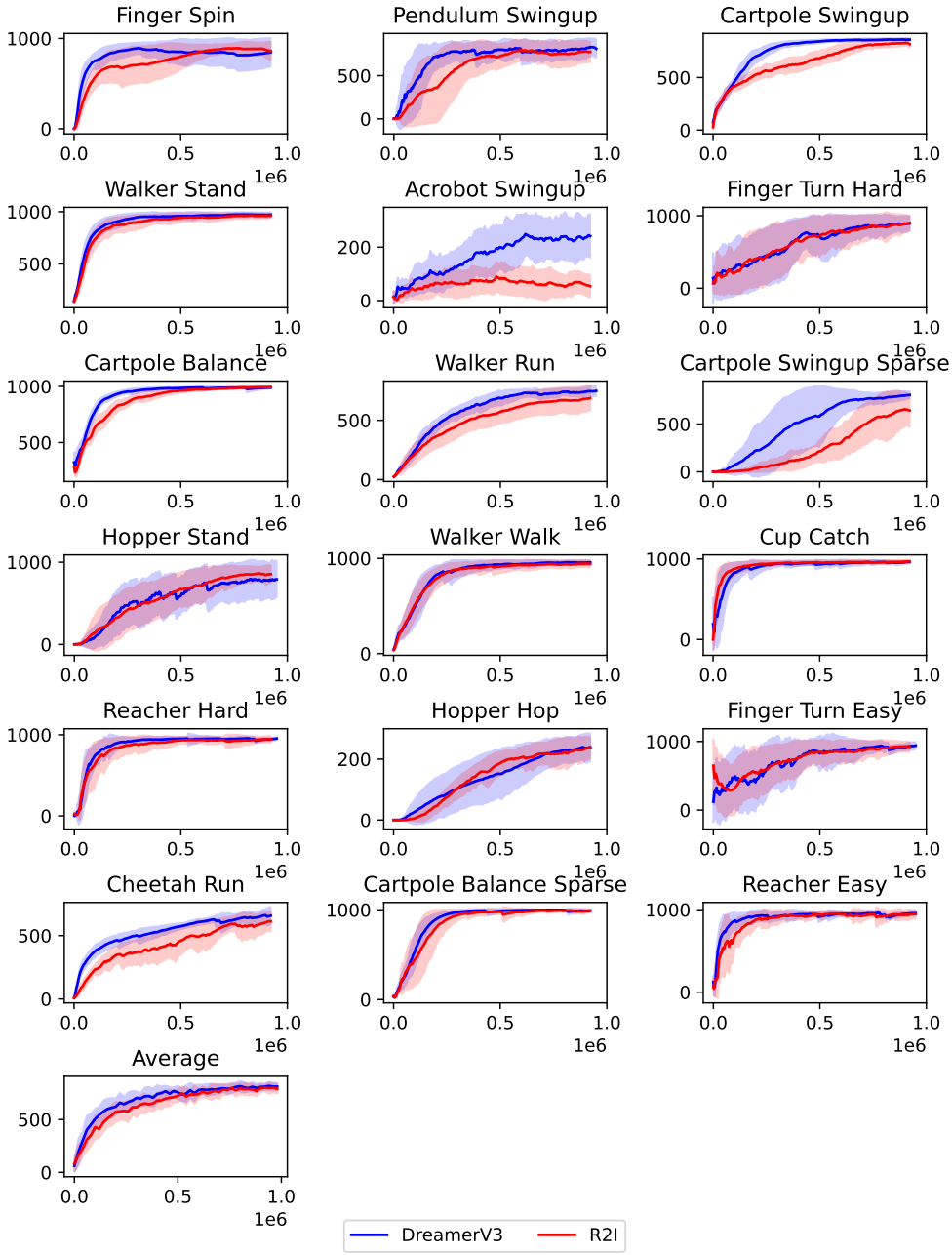

Figure 10: DMC-propreoceptive training curves. 3 seeds per run.

K DMC-VISION TRAINING CURVES

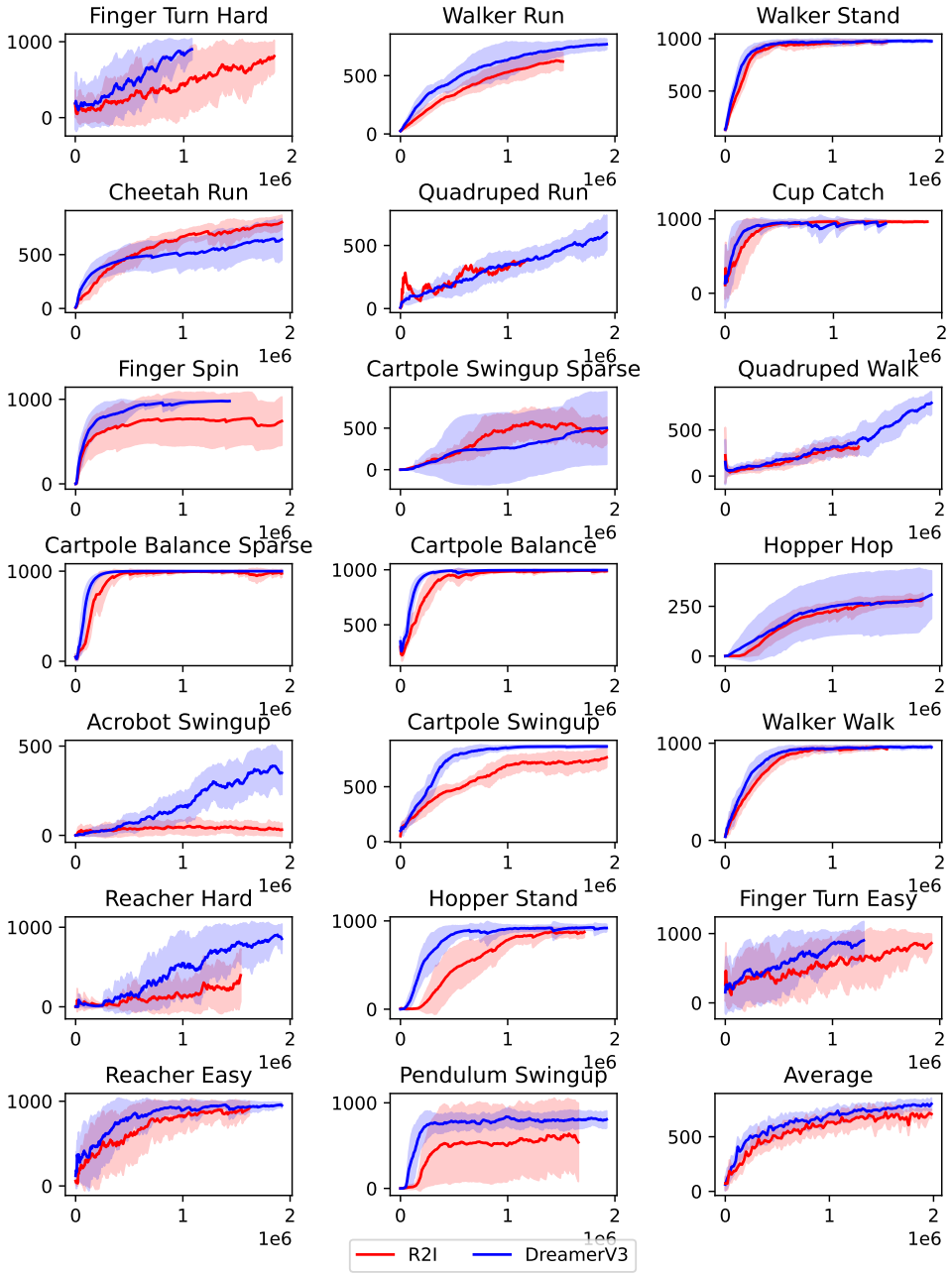

Figure 11: DMC scores for image inputs after 2M environment steps. 3 seeds per environment.

L Atari 100K Training Curves

Atari 100K benchmark (Łukasz Kaiser et al., 2020) is a standard RL benchmark comprising 26 Atari games featuring diverse gameplay mechanics. It is designed to assess a broad spectrum of agent skills, and agents are limited to executing 400 thousand discrete actions within each environment, which is approximately equivalent to 2 hours of human gameplay. To put this in perspective, when there are no constraints on sample efficiency, the typical practice is to train agents for almost 200M steps.

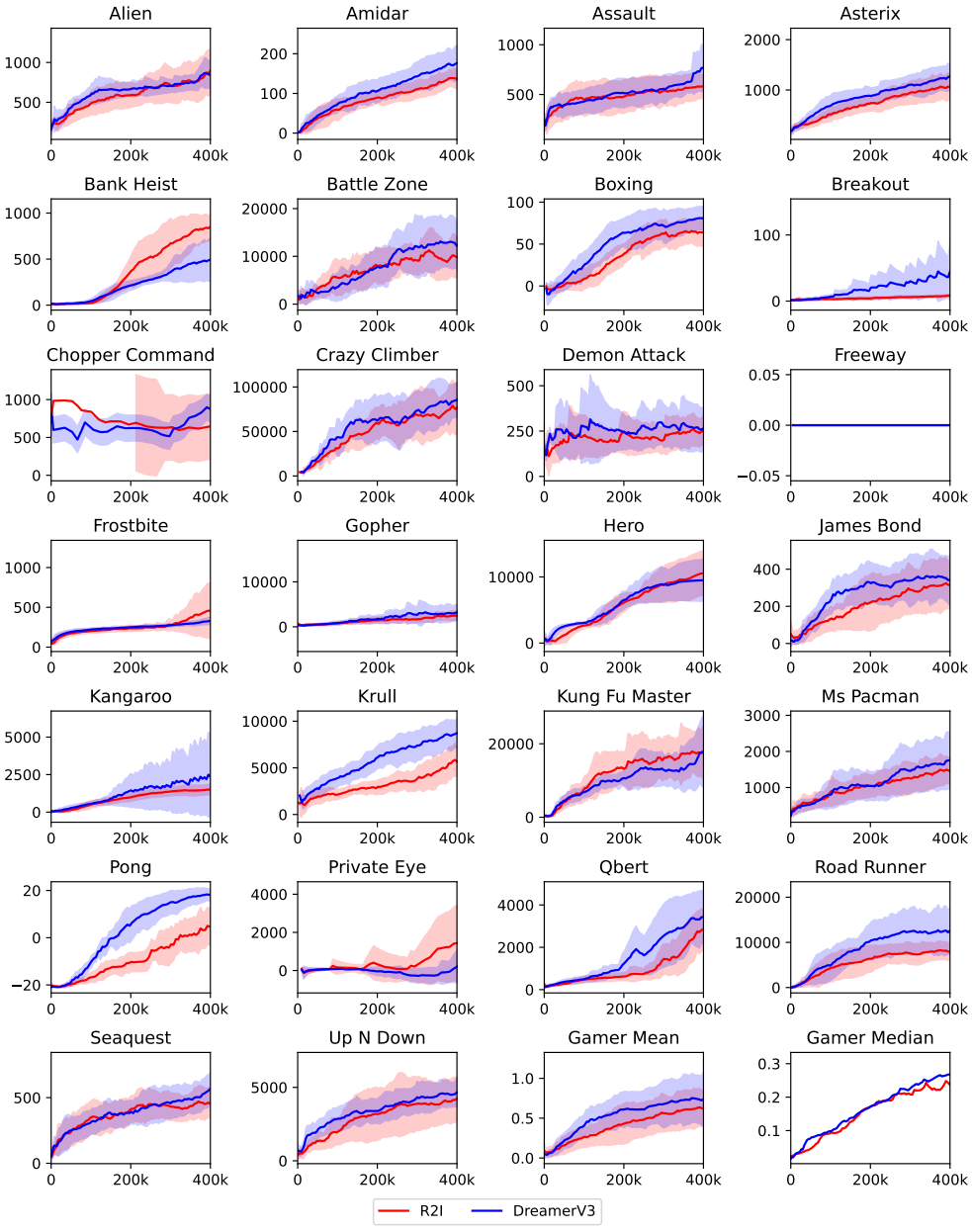

Figure 12: Atari scores after 400K environment steps. 3 seeds per environment.

M HYPERPARAMETER TUNING IN POPGYM

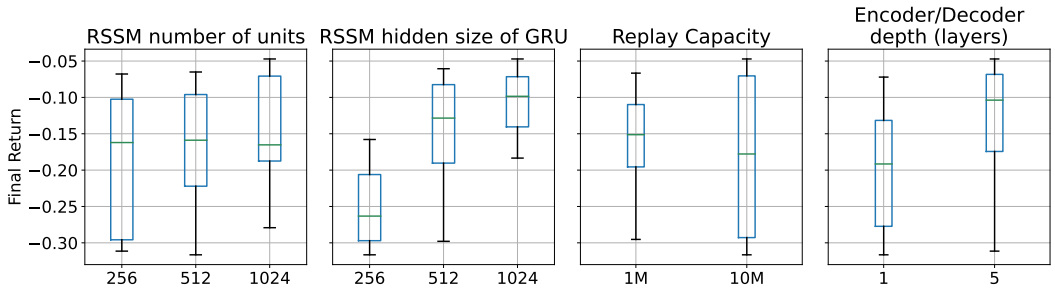

Figure 13: Results of hyperparameter tuning for DreamerV3 in POPGym memory environments.

To find a good baseline configuration to compare with, we performed hyperparameter tuning of the baseline DreamerV3 model. The results are shown in Figure 13. Each hyperparameter configuration of DreamerV3 was trained on 9 memory tasks from POPGym[3] considered in this study. To tune the model, we considered the following hyperparameters: 1) *number of units in RSSM*, that is, the sizes of auxiliary layers of RSSM, ranging in $\{256, 512, 1024\}$; 2) *hidden size of GRU in RSSM* ranging in $\{256, 512, 1024\}$; 3) *replay buffer size* – two values $\{10^6, 10^7\}$; 4) *sizes of encoder and decoder*. Each hyperparameter configuration was trained with two random seeds for 10 million environment steps. These choices are motivated in the following way. DreamerV3 was proposed as a general agent with all hyperparameters fixed except network sizes and training intensity, which control sample efficiency. To find a configuration that works the best, we chose to tune the model sizes ranging them around the configuration that was proposed for Behavior Suite (since POPGym and Behavior Suite share similar properties). We also checked an increased replay buffer size of 10M steps (besides standard 1M of DreamerV3) since it improved the performance for R2I.

Figure 13 shows a box plot for each hyperparameter with the marginal performance of each hyperparameter (i.e. for hyperparameter X, we fix X but vary all other hyperparameters, which form an empirical distribution with some median, max, min, etc.; we plot a box plot of empirical distribution for each X). This visualization shows how much each hyperparameter can contribute to the overall performance (as it shows the median with all other hyperparameters varied but a chosen one fixed) and also what is the best hyperparameter value for the task (since the box plot shows the maximal value). Our results confirm the favorable scaling of the DreamerV3 (Hafner et al., 2023) in this new environment – bigger networks learn bigger rewards. Therefore, we opt for 1024 RSSM units, RSSM hidden size of 1024, and 5 layers of encoder/decoder. Unlike for R2I, for DreamerV3, a bigger replay performs less "stable" – since it has bigger variation, e.g. increasing the network size might have an unexpected influence on the final agent performance. Yet, since with 10 million steps the model has the best score, we opt to this option for a fair comparison. The final DreamerV3 model reported in Figure 4 was trained on the best found configuration.

[3] `RepeatPrevious`,`Autoencode`, `Concentration`, for each – three difficulties: `Easy`, `Medium`, `Hard`

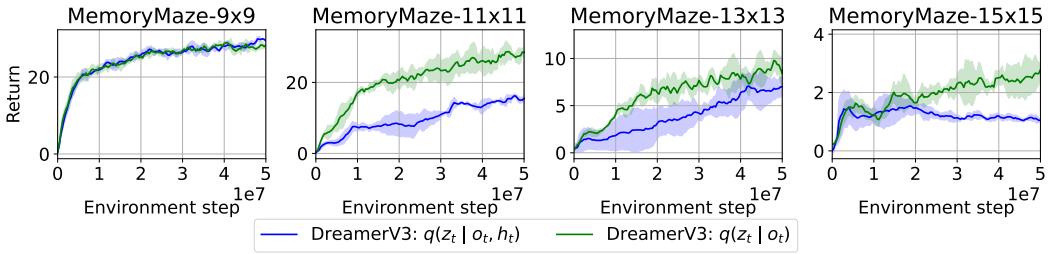

Figure 15: Recurrent and non-recurrent representation model ablation in Memory maze.

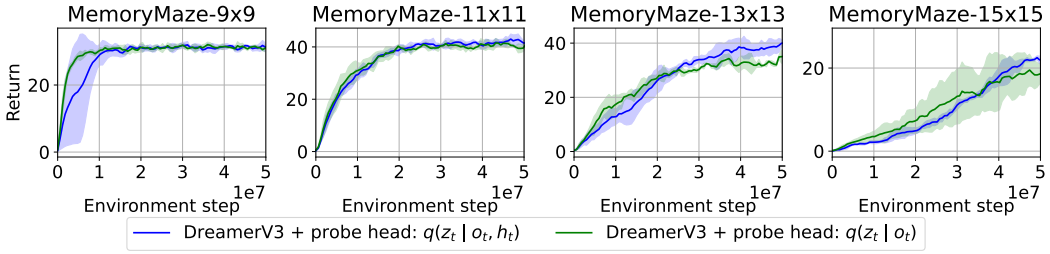

Figure 16: Recurrent and non-recurrent representation model ablation in Memory Maze with probing head.

N Impact of non-Recurrent Representation Model

In this section we study the impact of disconnecting the representation model from the sequence model. As discussed in Section 3, this disconnection is needed for the efficient computation of SSM sequence features in parallel (because otherwise, if the representation model's input needs the sequence model's previous output, the whole computation is inherently recurrent). Therefore, we study how important it is to keep this recurrent connection from the sequence model to the representation model.

First, we test how removing this recurrent connection afftect the performance in Memory Maze. We do so in two versions of this benchmark. The first one, is standard Memory Maze reported in this work. The second one is an extended version of the Memory Maze benchmark. This task adds additional information which is the target objects' coordinates. The agent is still given only an image as input, but now it is tasked to reconstruct both the input image and target positions (Pasukonis et al., 2022). As it is shown in Figures 15, 16, the non-recurrent representation model either keeps the performance the same or improves it. Note that when a probing network is used, the agent receives additional memory supervision (because it is tasked to predict target positions). Therefore, without memory supervision, the non-recurrent posterior improves performance, while with memory supervision it does not decrease it and keeps it the same. In other words, the non-recurrent representation model is an inductive bias that favors memory.

Lastly, as shown in Figure 14, in standards RL environments this recurrent connection has zero influence on performance, confirming that this inductive bias favors memory without any negative side effects.

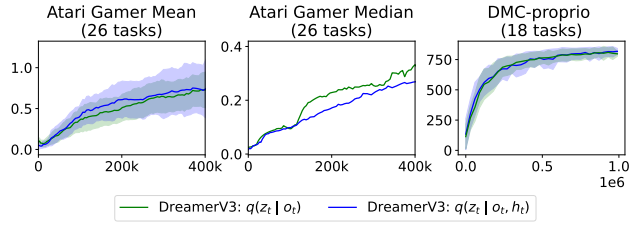

Figure 14: Recurrent and non-recurrent representation models in standard RL environments.

O Policy Input Ablations

In this section, we aim to answer the question "Which policy input variation works better?" As a reminder, S3M, a sequence models of R2I, has three main components exposed: deterministic output state h_t (is used to in prediction heads to summarize information from previous steps), stochastic state z_t (represents single observation), and hidden state x_t (is passed between time steps). The policy variants are output state policy $\pi(\hat{a}_t \mid z_t, h_t)$, hidden state policy $\pi(\hat{a}_t \mid z_t, x_t)$, full state policy $\pi(\hat{a}_t \mid z_t, h_t, x_t)$.

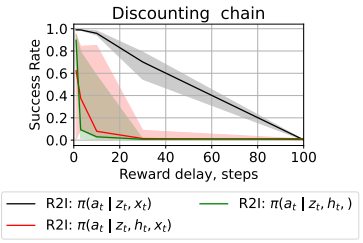

Figure 17: Actor-critic input ablations in discounting chain.

Our main insight is that in different environments h_t, z_t, and x_t behave differently and they may represent different information. At the same time, these features change their distribution along world model training, which makes the actor-critic training process less stable. Therefore, we found each domain has its own working configuration. The only shared trait is that memory environments typically require $\pi(\hat{a}_t \mid z_t, x_t)$ or $\pi(\hat{a}_t \mid z_t, h_t, x_t)$ to show strong performance (See Figure 17 and Figure 18). In Memory Maze, we found the effect of input features change is smaller. As Figure 19 shows, the output state policy performs worse than the other two.

However, there exists an extended version of the Memory Maze benchmark. This task adds additional information which is the target objects' coordinates. The agent is still given only an image as input, but now it is tasked to reconstruct both the input image and target positions (Pasukonis et al., 2022). As Figure 20 shares, all three policies converge to exactly the same reward values indicating there is no difference between (z_t, x_t) and (z_t, h_t).

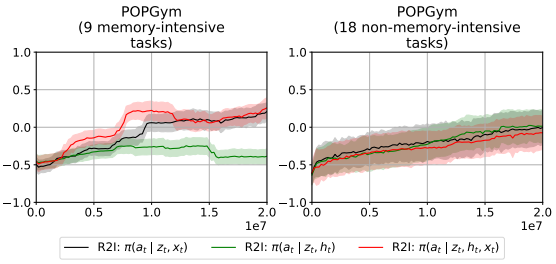

Figure 18: Actor-critic input ablations in POPGym.

Finally, as it is shown in Figure 21, policy input variations have little, yet non-zero influence on the final performance. This indicates that the information stored in (z_t, h_t) and (z_t, x_t) is mostly the same.

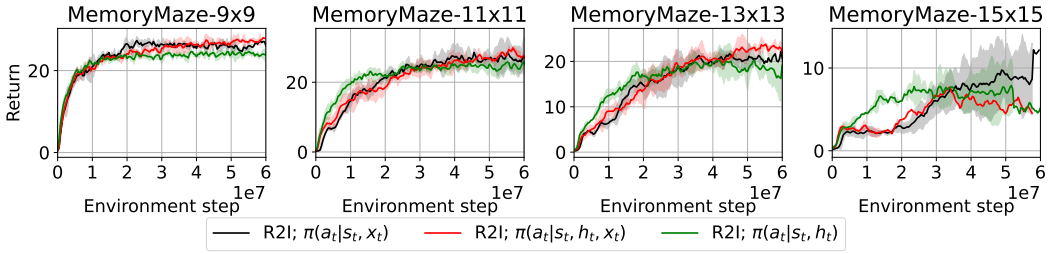

Figure 19: Memory maze policy ablations without probing heads. The performances of all three variants are qualitatively different indicating that the information in the S3M output h_t and S3M hidden x_t is different. In addition, the output state policy $\pi(\hat{a}_t \mid z_t, h_t)$ starts losing performance at some point.

[3]Non-memory-intensive environments include: `CountRecall`, `Battleship`, `MineSweeper`, `RepeatFirst`, `LabyrinthEscape`, `LabyrinthExplore`. All three difficulties (`Easy`, `Medium`, `Hard`) for each.

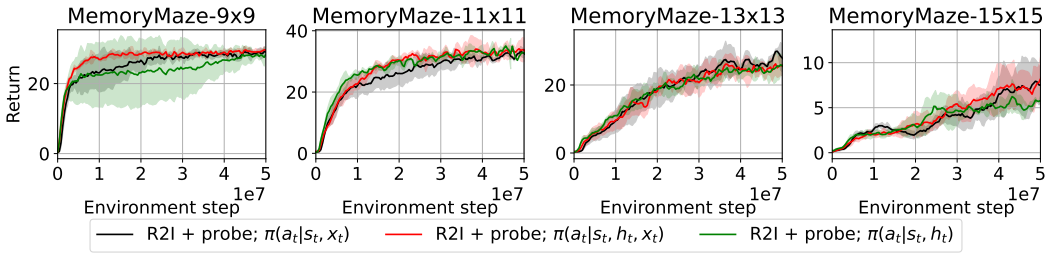

Figure 20: With probing head in Memory Maze, the agent is tasked to predict object locations from h_t (S3M output), effectively making h_t a markovian state (i.e. equivalent to hidden state x_t). Thus, we can see the performance of all three policy variants is effectively the same.

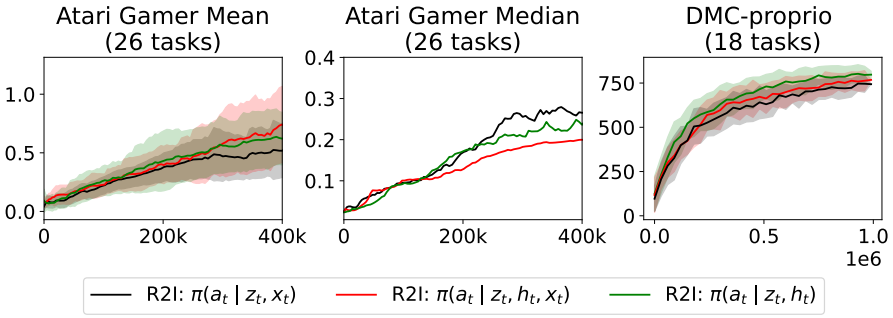

Figure 21: Actor-critic input ablations in Atari 100K and DMC domains.

P IMPORTANCE OF HAVING COMPLETE EPISODES IN TRAINING BATCH

In this section, we argue that it was a critical part of our model's success in memory tasks was to keep the sequence length in the batch big enough so that at least the entire RL episode fits into the batch as one sequence. Thanks to parallel scan (Blelloch, 1990) (see sections 2.1 and 3 for elaboration), the batch sequence length scales as efficiently as scaling the batch size, therefore, in all environments, we opt to train the model on complete episodes in the training batch.

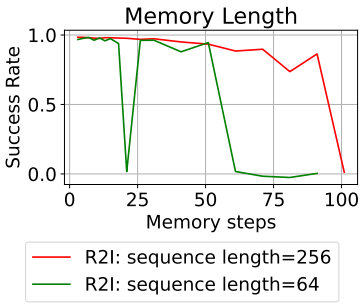

Figure 22: Actor-critic input ablations in discounting chain.

As shown in Figure 22, we train the model with the sequence length in batch equal to 64 and 256 steps. Over the x-axis, the episode length is varied and the agent is tasked to remember an observation and in the end, it is tasked to output a certain action associated with that first observation. When the episode length becomes greater than 64 steps, the performance becomes zero, while the model trained with 256 steps long batches keeps good performance as the episode length increases (since it is able to put the entire RL episode in training batch).

As shown in Figure 23 the performance scales positively with the sequence length. We test four different sequence lengths in batch with the R2I model: 64 steps, 128 steps, and 1024 steps. Along the scaling length, every step improves the performance indicating that the extended sequence length is required in memory tasks.

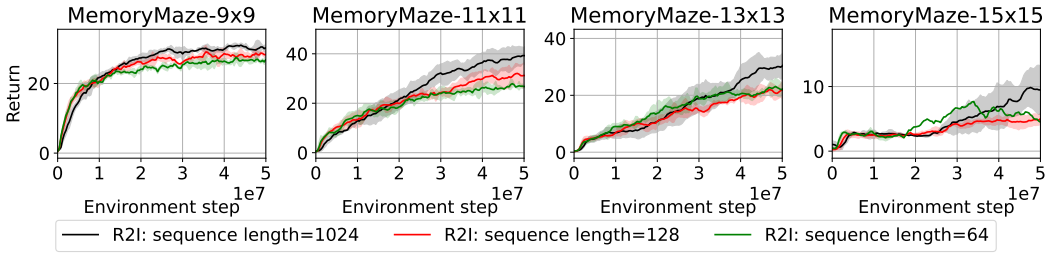

Figure 23: Length ablations.

Q Model Likelihood Relation with Agent Performance

In MBRL, the agent typically goes through a process of learning a world model and employs it for planning or optimizing the policy. Therefore, one might naturally assume a higher likelihood of the world model leads to improved policy performance. Nevertheless, this assumption does not hold true in all cases. When the world model has constrained representational capacity or its class is misspecified, its higher likelihood may not necessarily translate into better agent performance (Joseph et al., 2013; Lambert et al., 2020; Nikishin et al., 2021). In other words, the inaccuracies in the world model will only minimally affect the policy if it happens to be perfect. Conversely, in the case of an imperfect model, these inaccuracies can lead to subtle yet significant impacts on the agent's overall performance (Abbad, 1991). For example, Nikishin et al. (2021) propose a method wherein the model likelihood is less than a random baseline while the agent achieves higher returns. This implies that the learned world model may not always have to lead to predictions that closely align with the actual states, which are essential for optimizing policies.

Q.1 Comparing R2I with S4WM

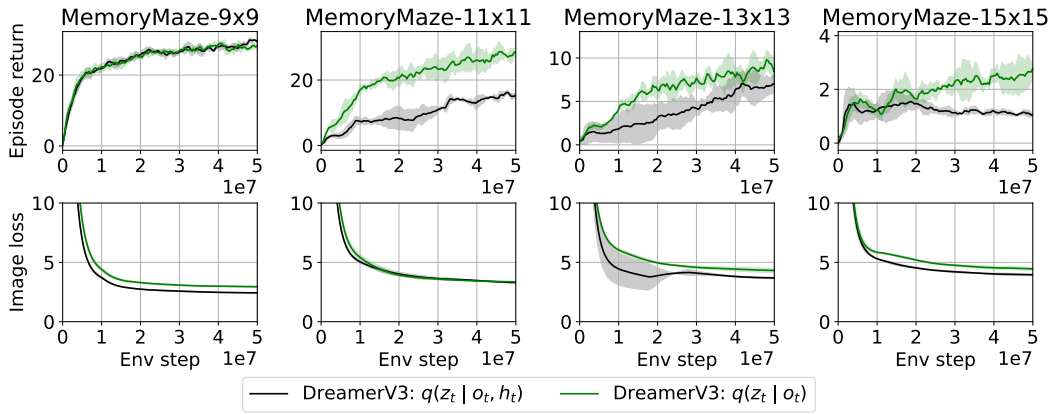

Figure 24: Online RL plots of the DreamerV3 model with recurrent and non-recurrent representation models (for details see Appendix N).

In parallel with our study, Deng et al. (2023) introduce a S4-based (Gu et al., 2021a) world model, called S4WM. The incorporation of S4 in the Dreamer world model has proven beneficial, as evidenced by the achievement of higher accuracy with lower Mean Squared Error (MSE). These results were obtained using offline datasets across various tabular environments and the Memory Maze (Pasukonis et al., 2022). However, their work primarily focuses on world modeling; for instance, there is no performance report in terms of obtained rewards. As previously discussed, a higher model likelihood does not necessarily guarantee better performance (i.e., higher rewards).

Figure 24 illustrates the results of DreamerV3 (which also serves as the predecessor to S4WM) with two distinct configurations for the world model on Memory Maze. One agent (depicted in green) incorporates a non-recurrent representation model, while the other (depicted in black) uses a recurrent one. Deng et al. (2023) utilize image loss as one of the key indicators for model likelihood. As shown, despite the agent with a non-recurrent representation model having a higher image loss, it manages to achieve higher rewards. This result is related to the experimental results of S4WM in the following manner. In S4WM, the authors conduct experiments with the datasets collected by scripted policies within environments like Memory Maze such as Four-rooms, Eight-rooms, and Ten-rooms. Also, they evaluate image generation metrics on a heldout dataset (compared to what the world model was trained on) to assess the in-context learning proficiency of the world model across unseen levels. Similarly, the outcomes depicted in Figure 24 provide online RL metrics within memory maze environments. It is noteworthy that here, the agent is trained with a replay buffer that is progressively updated. Therefore, successive batches may contain data from episodes within newly generated mazes that the model has not encountered before, reinforcing our assertion that these results are indeed comparable.

Table 5: Architectural comparison between R2I and S4WM

Feature	**R2I**	**S4WM**
Computational modeling	Parallel scan	Conv mode
Layer normalization	Postnorm	Prenorm
SSM in posterior and prior	Shared	Not shared[3]
Post-SSM transformation	GLU transformation	Linear transformation
SSM dimensionality	MIMO	SISO
SSM parameterization	Diagonal	DPLR
SSM discretization	Bilinear	? (Unspecified)
Handling resets technique	Reset to zero or learnable vectors	Not implemented
Exposure of hidden states	Provided by parallel scan	Not implemented
Policy training mode	DreamerV3's objective	None
World model objective	Same as DreamerV3	Same as DreamerV3 but without free info in KL
SSM block structure	SSM layer$\rightarrow$ $\rightarrow$ GLU $\rightarrow$ $\rightarrow$ LayerNorm	(LayerNorm $\rightarrow$ $\rightarrow$ SSM layer $\rightarrow$ $\rightarrow$ FC)$\times 2$ $\rightarrow$ $\rightarrow$ FC $\rightarrow$ LayerNorm

This highlights the idea that, in order to enhance long-term temporal reasoning in the context of MBRL and tackle memory-intensive tasks, simply maximizing world model likelihood is insufficient. That is why S4WM incorporates a completely different set of hyperparameters and design decisions, as detailed in Table 5. Here is a comprehensive explanation of each design decision that sets S4WM apart from R2I:

1. **Computational modeling.** R2I uses parallel scan (Blelloch, 1990; Smith et al., 2023) while S4WM uses global convolution (Gu et al., 2021a) for training. One difference between these two techniques is that parallel scan uses SSM to compute $u_{1:T}, x_0 \rightarrow y_{1:T}, x_{1:T}$ while convolution mode uses SSM to compute $u_{1:T}, x_0 \rightarrow y_{1:T}, x_T$. Yet, as discussed in Section 3.2 and empirically shown in Appendix O, providing the policy with the SSMs' hidden states $x_{1:T}$ is crucial for the agent's performance. This is not feasible with the convolution mode, as it does not yield these states.
2. **Layer normalization.** R2I applies post-normalization (i.e., after the SSM layers and right after the merge of the residual connections), whereas S4WM employs pre-normalization (i.e., before the SSM layer but subsequent to the residual branching). Pre-normalization tends to be more conducive for training models with significant depth, whereas post-normalization can offer a modest enhancement in generalization when a fewer number of layers are used (Wang et al., 2019). Given that our model must continuously generalize on data newly added to the replay buffer (as it performs online RL), post-normalization emerges as the more intuitive selection for Online RL. This choice is confirmed by our preliminary results.
3. **Shared SSM network.** R2I employs a shared SSM network for all prior prediction and posterior stochastic and deterministic models' inference, whereas S4WM investigates both shared and non-shared options, ultimately reporting the non-shared option as superior for image prediction. In this study, we have not explored the non-shared option; however, we anticipate that the non-shared version might prove less efficient for policy learning due to potential feature divergence between the posterior and prior SSM networks. This is because the policy is trained using features from the prior model but deployed in the environment with features from the posterior model.

[3]Here we refer to the S4WM-FullPosterior model. Even though it is not the main model, the S4WM-FullPosterior one showed superior image prediction performance.

4. **Post-SSM transformation.** R2I uses a GLU transformation (Dauphin et al., 2017), while S4WM uses a linear fully connected transformation. In our preliminary experiments, we explored both options and found that the GLU transformation yields better empirical results, particularly in terms of the expected return.
5. **SSM dimensionality.** R2I employs MIMO (Smith et al., 2023), while S4WM utilizes SISO (Gu et al., 2021a). Although the superiority of one over the other is not distinctly evident, MIMO provides more fine-grained control over the number of parameters in the SSM.
6. **SSM parameterization.** R2I adopts a diagonal parameterization (Gupta et al., 2022a) of the SSM, while S4WM employs a Diagonal-Plus-Low-Rank (DPLR) parameterization (Gu et al., 2021a). In our experiments, we found that both approaches perform comparably well in terms of agent performance. However, DPLR results in a significantly slower computation of imagination steps—approximately 2 to 3 times slower—therefore, we opted for the diagonal parameterization (See Appendix C.1.1).
7. **SSM discretization.** R2I utilizes bilinear discretization for its simplicity. S4WM does not specify the discretization method used; however, the standard choice for discretization within the S4 model typically relies on Woodbury's Identity (Gu et al., 2021a), which necessitates matrix inversion at every training step—a relatively costly operation. This is the reason we decided early on in this work not to proceed with S4.
8. **World model training objective.** R2I uses the same objective introduced in DreamerV3. In contrast, S4WM utilizes the ELBO objective in the formulation of DreamerV3, with the sole difference being that free information (Hafner et al., 2023) is not incorporated in the KL term. Notably, free information was introduced in DreamerV3 as a remedy to the policy overfitting (it is evidenced by the ablations in Hafner et al. (2023)).
9. **Episode reset handling technique.** R2I leverages the parallel scan operator introduced by Lu et al. (2023) and modifies it to allow a learnable or zero vector when an RL episode is reset, a technique that was introduced in DreamerV3. While S4WM is also based on the DreamerV3 framework, it overlooks this modification and lacks the mechanism to integrate episode boundaries into the training batch. This adaptation is critical under the non-stationarity of the policy being trained; it is primarily aimed at enhancing the efficiency of policy training; as the policy distribution changes, resulting in adjusted episode lengths, S4WM will be required to modify its sequence length accordingly—either increasing or decreasing it as necessary.

R A DEEPER COMPARISON BETWEEN DREAMERV3 AND R2I IN STANDARD RL BENCHMARKS

To facilitate a more comprehensive comparison between R2I and DreamerV3, we build performance profiles using the RLiable package (Agarwal et al., 2021). In particular, we use these profiles to illustrate the relationship between the distribution of final performances in R2I and DreamerV3, as depicted in Figure 25. In Atari 100K (Łukasz Kaiser et al., 2020) the performance profiles of DreamerV3 and R2I show remarkable similarity, indicating that their performance levels are almost identical. Looking at the proprioceptive and visual benchmarks in DMC (Tassa et al., 2018), we observe that R2I exhibits a drop in the fraction of runs with returns between 500 and 900. Outside of this interval, the difference between R2I and DreamerV3 diminishes significantly. Considering these observations, we conclude that R2I and DreamerV3 display comparable levels of performance across the majority of tested environments, aligning with our assertion that R2I does not compromise performance despite its enhanced memory capabilities. Note that this is a non-trivial property since these are significantly diverse environments, that feature continuous control (DMC), discrete control (Atari), stochastic dynamics (e.g., because of sticky actions of Atari), deterministic dynamics (in DMC), sparse rewards (e.g., there are several environments in DMC built specifically with an explicit reward sparsification), and dense rewards. Our findings confirm that the performance in the majority of these cases is preserved.

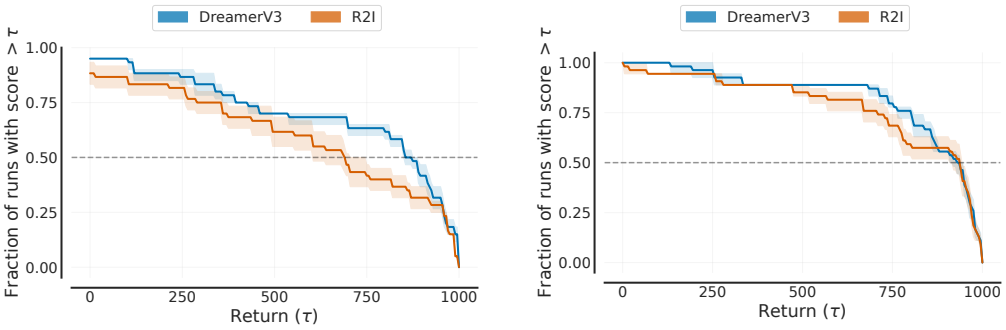

(a) Performance profiles in DMC-vision domain (20 Environments; 3 seeds per environment)

(b) Performance profiles in DMC-proprio (18 Environments; 3 seeds per environment)

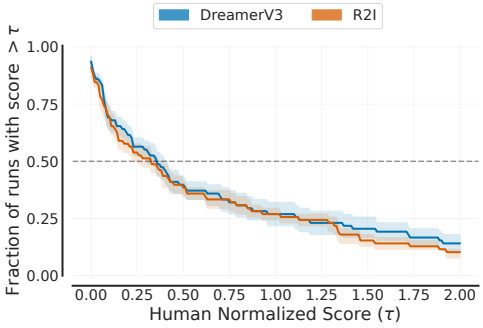

(c) Performance profiles in Atari100k (26 Environments; 3 seeds per environment)

Figure 25: Performance profiles of DreamerV3 and R2I evaluated in three RL domains: Atari100k,DMC-vision, DMC-proprio.

S ALGORITHM PSEUDOCODE

Algorithm 1: Recall to Imagine (R2I), full state policy training

Initialize empty FIFO Replay Buffer $\mathcal{D}$;
`// P is set to the total env. steps in batch to form at least one batch to start training`
Prefill $\mathcal{D}$ with P environment steps following the random policy;
while *not converged* **do**
  for *train step* $c = 1..C$ **do**
    `// World model training (parallel mode)`
    Draw n training trajectories $\{(a_t^j, o_t^j, r_t^j)\}_{t=k}^{k+L} = \tau_j \sim \mathcal{D},\ j = \overline{1,n}$;
    `// All variables are expected to include a batch dimension`
    `// which is omitted for simplicity`
    `// See Section 3.1`
    Encode observations batch $z_{1:T} \sim q_\theta(z_{1:T} \mid o_{1:T})$;
    Compute S3M hidden states and outputs with parallel scan
    $h_{1:T}, x_{1:T} \leftarrow f_\theta((a_{1:T}, z_{1:T}), x_0)$;
    `// Note that` $x_{1:T}$ `include hidden states from all SSM layers`
    Reconstruct rewards, observations, continue flags
    $\hat{r}_{1:T}, \hat{o}_{1:T}, \hat{c}_{1:T} \sim \prod_{t=1}^{T} p(o_t \mid z_t, h_t) p(r_t \mid z_t, h_t) p(c_t \mid z_t, h_t)$;
    Compute objective using Eq. (3), (4), (5), (6) and optimize WM parameters θ;
    `// Actor-critic training (recurrent mode)`
    `// See Section 2.2 and Appendix E for details`
    Initialize imagination $x_{0|1:T}, h_{0|1:T}, z_{0|1:T} \leftarrow x_{1:T}, h_{1:T}, z_{1:T}$;
    for *imagination step* $i = 0..H-1$ **do**
      $\hat{a}_{i|1:T} \sim \pi(\hat{a} \mid z_{i|1:T}, h_{i|1:T}, x_{i|1:T})$;
      `// Note that this is a one-step inference of SSM in recurrent mode`
      $h_{i+1|1:T}, x_{i+1|1:T} \leftarrow f_\phi((\hat{a}_{i|1:T}, z_{i|1:T}), x_{i|1:T})$;
      $\hat{z}_{i+1|1:T} \sim p_\theta(\hat{z} \mid h_{i+1|1:T})$;
      $\hat{r}_{i+1|1:T} \sim p(r \mid \hat{z}_{i+1|1:T}, h_{i+1|1:T})$;
      $\hat{c}_{i+1|1:T} \sim p(c \mid \hat{z}_{i+1|1:T}, h_{i+1|1:T})$
    end
    Estimate returns $R^\lambda_{1:H|1:T}$ using Eq. 8 and $\hat{c}_{1:H|1:T}, \hat{r}_{1:H|1:T}$;
    Update actor-critic using estimated returns according to the rule from Hafner et al. (2023);
  end
  Collect N steps in the environment using the World Model and the policy and store it to $\mathcal{D}$;
  `// the ratio` C/N `is training intensity which should be chosen according to the desired data-efficiency`
end

Algorithm 1 presents the pseudo-code for training the R2I in an online RL fashion. Note that the imagination phase is initialized from every possible step in the training batch. For example, $\hat{h}1 : H \mid 1 : T$ is a tensor of shape `[batch_size, T, H, dim]`, which represents the imagination output after 1 to H imagination steps starting from every possible time point (in total, there are T of them). This concept was initially proposed by Dreamer (Hafner et al., 2019a) and subsequently adopted by DreamerV2 (Hafner et al., 2020) and DreamerV3 (Hafner et al., 2023). We employ the same idea since the hidden states of the SSM are outputted by the parallel scan algorithm, allowing the use of all hidden states to compute imagination steps.

T MODEL-FREE SSM IN POPGYM

Figure 4 presents the performance of both model-free and model-based approaches in the most memory-intensive environments in POPGym (Morad et al., 2023). In terms of model-based methodologies, Dreamer is included, while model-free baselines comprise Proximal Policy Optimization (PPO; Schulman et al. (2017)) executed with a variety of network architectures, such as MLP, GRU, LSTM, and S4D (Gu et al., 2022). S4D stands as an SSM approach characterized by a SISO framework (Gu et al., 2021a), a diagonal parameterization for its SSM, and an efficient convolution mode for parallelization. The primary distinction between S4 (Gu et al., 2021a) and S4D lies in their parameterization methods; S4D's diagonal approach, as opposed to S4's DPLR parameterization, which makes S4D faster and potentially more stable.

According to the findings reported in the POPGym paper (Morad et al., 2023), the `PPO+S4D` configuration emerged as the least performant among the thirteen model-free baselines. It frequently encountered numerical difficulties such as not-a-numbers (NaNs), which can be attributed to gradient explosions. Please note that due to S4D's reliance on convolution mode, it is incapable of managing multiple episodes within a sequence.